266 566

A LIFTING SURFACE THEORY

FOR

WINGS EXTENDING THROUGH MULTIPLE JETS

T. Yao-tsu Wu
Richard B. Talmadge

Report No. 8 10 August 1961

Nonr 2388(00)

914

VEHICLE RESEARCH CORPORATION

PASADENA, CALIFORNIA

A LIFTING SURFACE THEORY

for

WINGS EXTENDING THROUGH MULTIPLE JETS

T. Yao-tsu Wu

Richard B. Talmadge

Conducted for

THE OFFICE OF NAVAL RESEARCH

under

Contract No. Nonr 2388(00)

VRC Report No. 8

10 August 1961

VEHICLE RESEARCH CORPORATION

1661 Lombardy Road
Pasadena, California

SYcamore 3-2695

FOREWORD

This report consists of the second phase of an analytical program to provide fundamental solutions to the non-uniform flow fields of wing-propeller aerodynamics. This program was originated by Dr. Scott Rethorst as an extension of his basic lifting surface solution obtained in an earlier study conducted at the California Institute of Technology.[1]

The program was formulated so that the effects of primary variables such as wing plan form were first determined. The analysis is then extended in order of increasing complexity to enhance its generality and to encompass secondary features. Each phase of the program establishes the foundation for the succeeding phases in an orderly growth pattern. The following four phases constitute the basic analytical portion of this program:

1. Single Jet Theory - The Rethorst analysis of Ref. 1 was applied to an extensive systematic spectrum of 437 wings. Optimum finite wing planforms were determined.[2]

2. Multiple Jet Theory - The single jet theory is further generalized and applied to the case of multiple jets. The effect of slip-stream rotation is also included. (Present Report).

3. High Angle of Attack Theory - The generalized theory is applied to analyses of (1) wings located at various heights in the jet, (2) highly cambered wings as used in deflected slipstream V/STOL concepts, and (3) tilt wing configurations where the jet is at an angle to the free stream flow.[3]

4. Separated Flow Theory - Hydrodynamic cavitation theory

is used to determine the separated flow field incurred during the transitional flight of V/STOL aircraft.[4]

The original Rethorst analysis of a wing extending through a single jet as used in Phase 1 employs an infinitesimal vortex element, which early in the analysis was integrated over a finite span element. The wing was then represented by a series of such finite spanwise horseshoe vortex elements.

Each such horseshoe vortex element was then split into components which were even and odd with respect to the direction of flow. The flow field due to the two dimensional even component was found in a straightforward algebraic manner. The flow field due to the three dimensional odd component is quite complex, involving infinite sums of infinite integrals of Bessel functions. Electronic data processing equipment is necessary for evaluation of these quadratures.

The present paper, in extending the Rethorst analysis to multiple jets, introduces four further significant refinements. First, the infinitesimal vortex elements are retained throughout the analysis, delaying the integration over the span until a final step. This technique simplifies the analysis and improves the accuracy of the results. Second, the symmetry restrictions have been removed so that more generalized geometries may be analyzed. Third, the odd component has been further partitioned into a simple algebraic component plus a complex remainder containing all of the Bessel function terms. If this remainder can be bounded and shown to be small enough to be disregarded, even in certain special cases, a major saving in computation will be achieved. Fourth, the effects of slipstream rotation have been included as a super-imposed element.

SUMMARY

The basic Rethorst lifting surface solution of a wing extending through a single jet was generalized to enhance its applicability to the solution of many general and secondary problems concerned with the non-uniform aerodynamics of wing-propeller interaction. The generalization is first developed in detail in terms of single jet theory. Then it is applied to multi-jet arrangements.

Several significant refinements to the original Rethorst theory are introduced. The wing is represented by a distribution of infinitesimal vortex elements instead of a large but finite number of horseshoe vortices. Certain symmetry restrictions are removed and the effect of slipstream rotation is included.

The spanwise lift distribution of an example multi-jet arrangement was determined. Large increases in lift inboard and within the jets were obtained when the free stream velocity was small compared to the jet velocity. A lesser but significant increase occurred outboard of the jets.

This large lift magnification offers the potential of large improvements in STOL capabilities and warrants a further computational effort which is presently being conducted.

TABLE OF CONTENTS

I. INTRODUCTION

The problem of the spanwise lift distribution on a wing of finite aspect-ratio extending through a central jet slipstream has been investigated by several authors. Koning[5] first treated this problem, using the lifting line theory together with certain simplifying assumptions. In Koning's work, the slipstream is taken to be a circular jet of air moving with a uniform velocity parallel to the main stream. The distortion of the slipstream due to the presence of the wing is assumed to be small so that the boundary conditions on the jet boundary may be applied, by linearization, at its undisturbed position. Furthermore, the difference between the jet velocity and the main flow velocity is assumed small; this limitation was introduced primarily to simplify the method of calculation used by Koning. Recently Koning's theory has been extended to render results valid for all jet velocities (with the other original assumptions retained) by Graham, Lagerstrom, Licher and Beane.[6].

The lift distribution along a wing of finite span with a central jet has been calculated by Squire and Chester[7], using the lifting line theory together with a rather elaborate expansion of the circulation distribution along the wing. Although the lifting line approximation well represents a wing of high aspect-ratio in a uniform main flow, the same approximation adapted to the present problem will further require that the slipstream diameter be large compared with the wing chord. In practice, however, the slipstream diameter and the chord are usually of the same order in magnitude. The applicability of the lifting line theory is therefore not well established.

On the other hand, if the slipstream diameter is small compared with the wing chord, the lift increase due to the jet effect is produced mainly over a low aspect-ratio surface, namely the portion of the wing in the jet and its immediate neighborhood. This special case has been treated by applying the slender body theory in Ref. 6. In this theory the basic velocity potential ϕ_B of the wing alone without the jet is considered as known and the jet perturbation potential $\Delta\phi = \phi - \phi_B$ is assumed to satisfy the slender body approximations; the problem of $\Delta\phi$ is then solved with the effect of finite aspect-ratio on $\Delta\phi$ neglected.

Judging from the different assumptions inherent in these two theories, it is expected that the lifting line theory will be valid for large values of the ratio of jet diameter to wing chord, whereas the slender body theory will be valid for small values of this ratio. In order to ascertain the range of validity of these two theories, their results have been compared in Ref. 6 for a particular example (a wing with sinusoidally varying incidence along the span, extending through a plane-sided free jet of finite width and infinite height) with the result of a third method, namely the approximate lifting surface theory of Weissinger[8].

The comparison shows that, at least for this particular case, the slender body theory is in good agreement with the lifting surface theory when the jet width is less than the wing chord. The lifting line theory is inadequate in this range of width-to-chord ratio, but in the limit tends to the Weissinger theory for large values of this ratio (about 10 or larger). While this finding indicates the range of validity of the two limiting theories in this special case, their respective ranges of validity in the general case, however, are not definitely established, as indicated by the comparison (given below) of their results with the existing experimental data.

For the general case it seems evident that some kind of lifting surface theory would be required to describe properly the actual flow. Based on this point of view, Rethorst[1] treated the original Koning problem by using the Weissinger approximation. In this analysis, the wing is represented by a large number of horseshoe vortices, which are obtained by integration of an infinitesimal vortex over a small but finite span element. The problem is then solved by the finite step method. To avoid the difficulties encountered in evaluating the convergence of the solution at the jet boundary, no vortex is chosen to stride across the jet boundary. This arrangement simplifies the boundary condition on the downwash at the intersection of the jet boundary and the wing. The lift distribution given by Rethorst's theory is shown to lie between the two limiting theories[1]. This theory of Rethorst has been subsequently applied to compute various flow quantities for a wide range of the velocity ratio (main stream velocity to jet velocity) and the ratio of jet diameter to chord; the results are reported in Ref. 2.

There are only a few experimental results on this slipstream problem. A series of experiments were conducted by Smelt and Davies[9], using a rectangular wing held at an incidence of 6.6 degrees, and with the propeller axis parallel to the main flow. Only the aerodynamic forces on the wing itself were measured. Compared with this set of experiments, the lift increment predicted by the slender body theory is about 30% lower than the experimental value[6], whereas the lift increment given by the lifting line theory is more than double the experimental data.

In a set of experiments carried out by Stuper[10], the spanwise lift distribution on a rectangular wing was measured at two angles of attack. A specially designed propeller was used to produce a jet with nearly uniform velocity distribution and without rotation. A comparison[1] shows that the experimental lift distribution of Stuper lies between the two limiting theories, whereas Rethorst's theory is found in substantial agreement with the experiment within the jet. Outside the jet, the correlation is obscured by the use of an upstream duct in Stuper's experiment.

Another experimental study of this problem was made recently by Brenckman[11]. It was found that within a range of moderate wing incidences, a substantial part of the lift increment produced by the slipstream is attributed to a destalling or boundary-layer-control effect. With this part of the lift increment deducted, the remaining part was found in good agreement with the slender body theory. The slipstream velocity profile (deviation from a uniform distribution), rotation, and deformation (from its original circular shape) were claimed to be of secondary importance. However, no apparent attempt was mentioned in Brenckman's investigation to examine the case when the angle of attack is so small that the destalling effect is practically absent, and to examine the other ranges of the chord-to-diameter ratio. Thus it seems that further experimental investigation of these points would be required in order to provide a more sound basis for comparison between the different theories and experiments.

More recently an extensive experimental investigation of the slipstream problem was undertaken at Princeton University, Department of Aeronautical Engineering. The first report of this work is on finite spans[12] and produced experimental data that was in close agreement with the Rethorst theory.

A further recent Princeton report on this program dealt with infinite aspect ratio wings[13]. The Rethorst formulation again proved to yield the best correlation with experimental results.

This Princeton program provides substantial experimental evidence of the validity of the present theoretical program, particularly the first phase based on Rethorst's work. This favorable correlation lends encouragement to the present generalization of this initial effort.

The present study is concerned mainly with the generalization of the Rethorst lifting surface theory so that the analysis may be more readily applied to an extensive set of general problems, such as multiple jets, slipstream rotation, ground effect, and the optimum wing form for total lift. The first two problems are solved in the present paper.

Because the Weissinger method is less time-consuming than other more elaborate lifting surface theories, it is adopted here as a first approximation to the lifting surface theory. In order to simplify the analysis and to improve the accuracy of the results, the wing is represented by a piece-wise continuous distribution of circulation Γ, which may admit a step-jump only at the jet boundaries. The circulation distribution Γ is further expressed by different Fourier series in different regions (inside and outside the jets) over the wing. With this expansion of Γ the condition that the downwash at the jet boundaries must be bounded can easily be enforced. The first few Fourier coefficients are determined by applying a number of boundary conditions at approximate points on the wing.

The case of a single jet is first considered in detail; the analysis is then generalized to the case of multiple jets. The effect of the slipstream rotation is accounted for in an approximate manner.

II. ANALYSIS

A. GENERAL FORMULATION

In this analytical treatment of the effect of a number of slipstreams on the spanwise lift distribution over a wing, the following simplifying assumptions are introduced. Each slipstream is taken to be a jet of air which has a circular cross section and has its central axis parallel to the main stream surrounding the jets. To begin with, the slipstreams are assumed to have no rotation about their axes; the effect of small slipstream rotation will be approximately estimated later in the analysis. Thus the slipstream velocity and the main stream velocity are assumed to be originally uniform and constant, equal to V_j and V_o respectively. In this analysis the quantity $(V_j - V_o)/(V_j + V_o)$ need not be limited to be small. When $V_j >> V_o$, the effect of the slipstreams becomes predominant; consequently the assumption that the slipstreams are parallel to the main stream becomes less important and may thereby be relaxed to some extent. It may also be noted that for $V_j >> V_o$, the mixing region at the jet boundary due to the viscous effect will become appreciable; this real fluid effect, however, will be neglected. It should be mentioned that, as pointed out by Brenckman[11], a substantial part of the lift increment at moderate incident angles produced by the slipstream is attributed to a "destalling" effect which reduces the flow separation on account of the high velocity slipstream. This point of view would seem to require some kind of new or modified analysis, presumably with the use of the free streamline theory to represent the separated flow. Within the present framework, however, the flow is assumed to be free from separation

The flow is assumed to be incompressible and nonviscous, hence it possesses a velocity potential inside and outside the jet, though the potential need not be continuous at the jet boundary. The jet boundary may be regarded as a vortex sheet separating the inside and outside flow. The only other singularities are the vortex elements representing the wing and the trailing vortex sheet shed from the wing. The disturbances produced by the wing are assumed to fall off far away from the wing except, of course, along its trailing vortex sheet.

Before the analysis is extended to the case of multiple jets, we consider first the case of a single circular jet, with its radius normalized to unity for simplicity. The jet axis is taken to be the x-axis, directed along the main flow and centered at the wing chord. The wing extends through the jet, spanning from $y = -b_1$ to $y = +b_2$ ($b_1, b_2 > 1$, see Fig. 1). The z-axis is taken to point upward. The ratio between the main stream velocity V_o and the jet velocity V_j will be denoted by

$$\mu = V_o/V_j, \quad 0 \leq \mu \leq 1 . \tag{1}$$

The perturbation velocity potential outside and inside the jet will be denoted by φ_o and φ_j so that the total velocity will be respectively

$$\vec{q}_o = V_o\vec{i} + \text{grad}\,\varphi_o, \quad \vec{q}_j = V_j\vec{i} + \text{grad}\,\varphi_j \tag{2}$$

where $\vec{i}$ is a unit vector along the x-axis. In their respective flow regions φ_o and φ_j satisfy the Laplace equation

$$\nabla^2\varphi_o = 0, \qquad \nabla^2\varphi_j = 0 . \tag{3}$$

The distortion of the slipstream by the wing is assumed small so that by linearization, the conditions on the jet boundary may be applied on the original circular free boundary. There are two boundary conditions at the jet boundary. One of them is dynamic in nature, stating that the pressure must be continuous at the jet boundary; that is,[5]

$$\varphi_j = \mu\varphi_o \quad \text{on} \quad r = (y^2 + z^2)^{1/2} = 1 \ . \tag{4}$$

The other condition, kinematic in nature, expresses that the inside and outside flow must be tangential to each other at the boundary, that is,

$$\partial\varphi_o/\partial r = \mu\partial\varphi_j/\partial r \quad \text{on} \quad r = 1 \ . \tag{5}$$

The boundary conditions on the trailing vortex sheet of the wing will be described below (immediately after Eq. 6), and the boundary condition on the lifting surface representing the wing will be given later in this analysis (see Section B4).

In order to generalize the analysis and to improve its accuracy for subsequent numerical computations, the wing will be represented by a distribution of infinitesimal vortex elements instead of a number of finite horseshoe vortices as in Ref. 1. Let us first consider an infinitesimal element of bound vortex of strength $\Gamma(\eta)\delta\eta$ centered at $x = 0$, $y = \eta$, $z = 0$, and extending over a line element $\delta\eta$ along the y-axis, the free stream being everywhere uniform, of velocity V in the positive x-direction. The trailing vortex sheet of this bound vortex element lies approximately in the region $x > 0$, $\eta - \delta\eta/2 < y < \eta + \delta\eta/2$, $z = 0$. The solution of this problem is well known (e. g. see Ref. 14); it may be expressed as

$$\delta\varphi = \delta\varphi_1 + \delta\varphi_2 = \frac{1}{4\pi}\,\Gamma(\eta)\delta\eta[\,F_1(y-\eta, z) + F_2(x, y-\eta, z)], \tag{6a}$$

where

$$F_1(y, z) = \frac{z}{y^2 + z^2} \tag{6b}$$

$$F_2(x, y, z) = z \int_0^x \frac{d\xi}{(\xi^2 + y^2 + z^2)^{3/2}}$$

$$= \frac{z}{y^2 + z^2} \frac{x}{(x^2 + y^2 + z^2)^{1/2}} \ . \tag{6c}$$

This solution is seen to satisfy the Laplace equation and to have the following properties:

1. Across the trailing vortex sheet $|y-\eta| < \delta\eta/2$, $x > 0$, $z = 0$, the potential $\delta\varphi$ has a jump $\delta\varphi(x, y, 0+) - \delta\varphi(x, y, 0-) = \Gamma(\eta)\delta\eta$, and $\delta\varphi(x, y, 0) = 0$ elsewhere.
2. Across the trailing vortex sheet $\delta\varphi_x$, $\delta\varphi_z$ are continuous and $\delta\varphi_y$ may be discontinuous, but $(\delta\varphi_y)^2$ is continuous.
3. $\delta\varphi \to 0$ as $x^2 + y^2 + z^2 \to \infty$ except over the vortex sheet.

Here $\delta\varphi$ is conveniently decomposed into two parts, $\delta\varphi_1$ and $\delta\varphi_2$. The part $\delta\varphi_1$ is independent of x, and will be called the two-dimensional part of the potential. The part $\delta\varphi_2$ is a function which is odd in x and z, but even in $(y-\eta)$, and will be called the three-dimensional part of the potential. The whole part $\delta\varphi$ may be regarded as the fundamental solution of a vortex element, and is useful in constructing the solution of more complicated boundary value problems. By using this fundamental solution, the velocity field generated by a distribution of circulation $\Gamma(y)$ along the wing span $(-b_1 < y < b_2)$ under the influence of a single jet can readily be calculated; this is given in the next section. This result will be further generalized to the case of multiple jets. Finally, the approximate lifting surface theory of Weissinger will be applied by taking one or more of such lifting lines appropriately distributed over the wing surface to represent the wing together with appropriate boundary conditions to ensure that the wing remains a rigid surface.

B. SINGLE JET THEORY

1. The Velocity Potential of a Lifting Line Extending through a Single Jet

We shall first derive from the above fundamental solution Eq. (6) the velocity potential of an infinitesimal bound vortex of strength $\Gamma(\eta)\delta\eta$ placed at $(0, \eta, 0)$ in the presence of a single jet with its boundary at $r = 1$. This solution may further be regarded as the fundamental solution, or the Green's function, of the wing-jet interference problem. It turns out that the determination of this Green's function depends on whether the vortex element is located inside or outside the jet slipstream. The velocity potential of a whole lifting line extending through the jet can then be obtained by superposition of this Green's function. We shall consider the two-dimensional and the three-dimensional part of the solution separately.

a. Two-dimensional Part of the Velocity Potential

The two-dimensional part of the velocity potential can be readily derived from Eq. (6) by making use of the simple reflection into the circular jet boundary, as given in Koning's theory[5]. The following two different cases must be distinguished.

(1) $|\eta| > 1$, the Vortex Element is located Outside the Slipstream

In this case it can be shown that the velocity potential outside the jet is due to the original vortex of strength $\Gamma(\eta)\delta\eta$ at $y = \eta$ plus an image vortex of strength $(1 - \mu^2)(1 + \mu^2)^{-1}\eta^{-2}\Gamma(\eta)\delta\eta$ at $y = 1/\eta$ (which is inside the jet). On the other hand, the velocity potential inside the jet is due to an equivalent vortex of strength $2\mu(1 + \mu^2)^{-1}\Gamma(\eta)\delta\eta$ located at the original position $y = \eta$. For brevity we write

$$\epsilon_1 = (1 - \mu^2)/(1 + \mu^2), \qquad \epsilon_2 = (1 - \mu)^2/(1 + \mu^2), \tag{7}$$

which also satisfy the relations

$$(1 - \epsilon_2) = (1 - \epsilon_1)/\mu = \mu(1 + \epsilon_1). \tag{7a}$$

Then

$$\begin{aligned} \delta\varphi_1 &= \frac{1}{4\pi}\Gamma(\eta)\delta\eta\{F_1(y-\eta, z) + \frac{\epsilon_1}{\eta^2}F_1(y-\frac{1}{\eta}, z)\} \qquad \text{for } r > 1, \\ &= \frac{1}{4\pi}\Gamma(\eta)\delta\eta(1 - \epsilon_2)F_1(y-\eta, z) \qquad \text{for } r < 1, \end{aligned} \tag{8}$$

where $r = (y^2 + z^2)^{1/2}$ and $F_1(y, z)$ is given by (6b). That this solution satisfies conditions (4) and (5) is readily verified by direct substitution. In the above expression the terms with ϵ_1 and ϵ_2 represent the effect of the slipstream on $\delta\varphi_1$ outside and inside the jet respectively. If the value of $\Gamma(\eta)$ is given, then it is seen at once from (8) that for a vortex element located outside the jet, the effect of the slipstream is to increase φ_1 outside the jet and to decrease φ_1 inside the jet.

(2) $|\eta| < 1$, the Vortex Element is located Inside the Slipstream

In this case it can also be shown that the velocity potential outside the jet is due to an equivalent vortex of strength $(1-\epsilon_2)\Gamma(\eta)\delta\eta$ located at $y = \eta$, and the potential inside the jet is due to the original vortex $\Gamma(\eta)\delta\eta$ at $y = \eta$ plus an image vortex of strength $-\epsilon_1\eta^{-2}\Gamma(\eta)\delta\eta$ located at $y = 1/\eta$ (which is outside the jet). That is

$$
\begin{aligned}
\delta\varphi_1 &= \frac{1}{4\pi}\Gamma(\eta)\delta\eta(1-\epsilon_2)F_1(y-\eta, z) && \text{for } r > 1, \\
&= \frac{1}{4\pi}\Gamma(\eta)\delta\eta\{F_1(y-\eta, z) - \frac{\epsilon_1}{\eta^2}F_1(y-\frac{1}{\eta}, z)\} && \text{for } r < 1.
\end{aligned}
\tag{9}
$$

This solution also satisfies conditions (4) and (5), as is readily verified. The effect of the jet slipstream is now to decrease the value of φ_1 both outside and inside the jet for fixed Γ.

The system of equations (8) and (9) represents the two-dimensional part of the Green's function of the wing-jet problem. For a lifting vortex line of a given circulation distribution $\Gamma(y)$ extending from $y = -b_1$ to $y = b_2$, the two-dimensional part of the velocity potential can be obtained, as the problem is evidently linear, by integrating (8) and (9) along the lifting line with the contributions in different regions kept in order. Thus we have

$$
\begin{aligned}
4\pi\varphi_1 = &\int_{-b_1}^{b_2} \Gamma(\eta)F_1(y-\eta, z)d\eta - \epsilon_2\int_{-1}^{1}\Gamma(\eta)F_1(y-\eta, z)d\eta \\
&+ \epsilon_1\left(\int_{-b_1}^{-1} + \int_{1}^{b_2}\right)\Gamma(\eta)F_1(y-\frac{1}{\eta}, z)\frac{d\eta}{\eta^2} \quad \text{for } r > 1,
\end{aligned}
\tag{10a}
$$

$$4\pi\varphi_1 = \int_{-b_1}^{b_2} \Gamma(\eta)F_1(y-\eta, z)d\eta - \epsilon_2\left(\int_{-b_1}^{-1} + \int_1^{b_2}\right)\Gamma(\eta)F_1(y-\eta, z)d\eta$$

$$- \epsilon_1\int_{-1}^{1} \Gamma(\eta)F_1(y-\frac{1}{\eta}, z)\frac{d\eta}{\eta^2} \qquad \text{for } r < 1. \qquad (10b)$$

b. Three-dimensional Part of the Velocity Potential

It has been found that the three-dimensional part of the velocity potential in the presence of a jet slipstream cannot be expressed in terms of the simple image system alone as for the two-dimensional part. However, by introducing the same image system as that of φ_1 to one part of φ_2 and by leaving the remaining part of φ_2 to be determined, the analysis can be somewhat simplified. We proceed as follows.

1. $|\eta| > 1$, with the Vortex Element located Outside the Jet

In this case we write φ_2 in the form which contains partly the same image system as that of (8) as follows

$$\delta\varphi_2 = \frac{1}{4\pi}\Gamma(\eta)\delta\eta\{F_2(x, y-\eta, z) + \frac{\epsilon_1}{\eta^2}F_2(x, y-\frac{1}{\eta}, z) + \varphi_o'\}$$

$$\text{for } r > 1, \qquad (11a)$$

$$= \frac{1}{4\pi}\Gamma(\eta)\delta\eta\{(1-\epsilon_2)F_2(x, y-\eta, z) + \varphi_j'\} \qquad \text{for } r < 1, \qquad (11b)$$

in which F_2 is defined in (6c) and φ_o' and φ_j' satisfy the Laplace equation and are to be determined by using conditions (4) and (5). For this purpose it is convenient to write the Laplace equation in polar coordinates (r, θ, x) with $r = (y^2 + z^2)^{1/2}$ and $\theta = \arctan(z/y)$, so that

$$\frac{\partial^2\varphi'}{\partial r^2} + \frac{1}{r}\frac{\partial\varphi'}{\partial r} + \frac{1}{r^2}\frac{\partial^2\varphi'}{\partial\theta^2} + \frac{\partial^2\varphi'}{\partial x^2} = 0 \qquad (12)$$

where $\varphi' = \varphi'_o$ for $r > 1$ and $\varphi' = \varphi'_j$ for $r < 1$. Substituting (11) into conditions (4) and (5), and using the integral representation of F_2 given in (6c), one obtains two boundary conditions for φ' as follows

$$(\varphi'_j - \mu\varphi'_o)_{r=1} = \mu\epsilon_1 \int_x^{|\eta| x} \frac{\sin\theta \, d\xi}{(\xi^2+\eta^2-2\eta\cos\theta+1)^{3/2}}, \tag{13}$$

$$\left(\frac{\partial\varphi'_o}{\partial r} - \mu\frac{\partial\varphi'_j}{\partial r}\right)_{r=1} = \epsilon_1 \left\{\frac{x\sin\theta}{(x^2+\eta^2-2\eta\cos\theta+1)^{3/2}} - \int_x^{|\eta| x} \frac{\partial}{\partial\eta}\left[\frac{\eta\sin\theta}{(\xi^2+\eta^2-2\eta\cos\theta+1)^{3/2}}\right] d\xi\right\}. \tag{14}$$

The above integrals can easily be integrated. By doing so, one may readily see that conditions (13) and (14) show that φ' has the following behavior

$$\varphi' = O(|x|) \text{ as } x \to 0, \quad \text{and} \quad \varphi' = O(x^{-2}) \text{ as } |x| \to \infty.$$

Hence φ' and its derivatives will be small both near $x = 0$ and $|x| = \infty$. This result exhibits the advantage of expressing φ_2 in the form (11), with the simple image system first singled out. Furthermore, (13) and (14) indicate that φ' will be a function odd in both x and θ. It therefore follows that φ' must be of the following form, which is readily verified to be a solution of (12),

$$\varphi' = \varphi'_o = \frac{2}{\pi}\sum_{n=1}^{\infty} \sin n\theta \int_0^{\infty} S_n^{(o)}(k,\eta) K_n(kr) \sin kx \, dk \quad \text{for } r > 1, \tag{15a}$$

$$= \varphi'_j = \frac{2}{\pi}\sum_{n=1}^{\infty} \sin n\theta \int_0^{\infty} S_n^{(j)}(k,\eta) I_n(kr) \sin kx \, dk \quad \text{for } r < 1, \tag{15b}$$

where I_n and K_n are the modified Bessel functions of the first and second kind, $S_n^{(o)}$ and $S_n^{(j)}$ are arbitrary functions of k and η. The functions K_n are chosen for $r > 1$ and I_n for $r < 1$ so that φ_o' and φ_j' will be regular respectively at $r = \infty$ and $r = 0$. The super-indices (o) and (j) of S denote the regions (outside or inside the jet) with which S is associated; this notation is convenient for extending the analysis to the case of multiple jets.

To facilitate the determination of $S_n^{(o)}$ and $S_n^{(j)}$, it is convenient to express conditions (13) and (14) also in terms of Fourier-Bessel integrals. By using the relations (which can be deduced from the results on p. 388 of Ref. 15)

$$\frac{x}{(x^2+\eta^2-2\eta\cos\theta+1)^{3/2}} = \frac{2}{\pi}\int_0^\infty K_o[k(\eta^2-2\eta\cos\theta+1)^{1/2}]\sin(kx)\,k\,dk, \tag{16a}$$

$$\int_x^{|\eta|x} \frac{d\xi}{(\xi^2+\eta^2-2\eta\cos\theta+1)^{3/2}}$$

$$= \frac{2}{\pi}\int_0^\infty \frac{\sin kx}{k}\,dk \int_{k/|\eta|}^{k} tK_o[t(\eta^2-2\eta\cos\theta+1)^{1/2}]\,dt, \tag{16b}$$

and the addition theorem (see Ref. 15, p. 361)

$$\sin\theta\, K_o[t(\eta^2-2\eta\cos\theta+1)^{1/2}]$$

$$= \sum_{n=1}^{\infty}[I_{n-1}(t)K_{n-1}(\eta t) - I_{n+1}(t)K_{n+1}(\eta t)]\sin n\theta \quad \text{for } |\eta| > 1, \tag{17a}$$

$$= \sum_{n=1}^{\infty}[I_{n-1}(\eta t)K_{n-1}(t) - I_{n+1}(\eta t)K_{n+1}(t)]\sin n\theta \quad \text{for } |\eta| < 1, \tag{17b}$$

together with the integral (which can be verified by differentiation)

$$\int [\, I_{n-1}(at)K_{n-1}(bt) - I_{n+1}(at)K_{n+1}(bt)]\, t\, dt$$

$$= -\frac{2n}{ab}\, I_n(at)K_n(bt), \tag{18}$$

one finds by straightforward calculation that (13) and (14) can be written

$$(\varphi_j' - \mu\varphi_o')_{r=1}$$

$$= \frac{4\mu\epsilon_1}{\pi\eta} \sum_{n=1}^{\infty} n \sin n\theta \int_0^{\infty} [\, I_n(\frac{k}{\eta})K_n(k) - I_n(k)K_n(k\eta)]\, \frac{\sin kx}{k}\, dk, \tag{19}$$

$$\left(\mu \frac{\partial\varphi_j'}{\partial r} - \frac{\partial\varphi_o'}{\partial r}\right)_{r=1}$$

$$= \frac{4\epsilon_1}{\pi\eta} \sum_{n=1}^{\infty} n \sin n\theta \int_0^{\infty} [\, I_n(\frac{k}{\eta})K_n'(k) + I_n'(k)K_n(k\eta)]\, \sin kx\, dk, \tag{20}$$

where I_n' and K_n' denote the derivatives of I_n and K_n with respect to their arguments.

A remark should be made here with regard to the argument of the Bessel functions when it becomes negative. Since the right-hand sides of (13), (14) and the left side of (17) are not changed if η is replaced by $(-\eta)$ and θ by $(\pi-\theta)$, the right side of (17a) and (17b) is also unchanged under the same transformation. Therefore we may adopt for the purpose of later calculation the conventions

$$K_n(-z) = (-)^n K_n(z), \qquad I_n(-z) = (-)^n I_n(z), \tag{21}$$

which are consistent at least for the present analysis.

Now application of conditions (19) and (20) to (15) yields

$$S_n^{(o)}(k,\eta) = \epsilon_1 \frac{2n}{\eta k}\left\{\frac{2kI_n I_n' K_n(k\eta)}{1-\epsilon_1 k(I_n K_n' + K_n I_n')} - I_n\left(\frac{k}{\eta}\right)\right\}, \tag{22a}$$

$$S_n^{(j)}(k,\eta) = \epsilon_1(1-\epsilon_2)\frac{2n}{\eta}\,\frac{[I_n K_n' + K_n I_n']\,K_n(k\eta)}{1-\epsilon_1 k(I_n K_n' + K_n I_n')}. \tag{22b}$$

In these equations, for those Bessel functions whose argument is k, the argument is omitted for brevity. Thus, Eqs. (11), (15) and (22) constitute the three-dimensional part of the Green's function for a vortex element located outside the jet.

(2) $|\eta| < 1$, with the Vortex Element located Inside the Jet

The solution of this case can be obtained by the same method as given in the previous section. The final result, as can be verified, is

$$\delta\varphi_2 = \frac{1}{4\pi}\Gamma(\eta)\delta\eta\{(1-\epsilon_2)F_2(x, y-\eta, z) + \varphi_o'\} \qquad \text{for } r > 1, \tag{23a}$$

$$\delta\varphi_2 = \frac{1}{4\pi}\Gamma(\eta)\delta\eta\{F_2(x, y-\eta, z) - \frac{\epsilon_1}{\eta^2}F_2(x, y-\frac{1}{\eta}, z) + \varphi_j'\} \qquad \text{for } r < 1; \tag{23b}$$

$$\varphi_o' = \frac{2}{\pi}\sum_{n=1}^{\infty}\sin n\theta\int_0^{\infty} T_n^{(o)}(k,\eta)K_n(kr)\sin kx\,dk \qquad \text{for } r > 1 \tag{24a}$$

$$\varphi_j' = \frac{2}{\pi}\sum_{n=1}^{\infty}\sin n\theta\int_0^{\infty} T_n^{(j)}(k,\eta)I_n(kr)\sin kx\,dk \qquad \text{for } r < 1; \tag{24b}$$

and

$$T_n^{(o)}(k,\eta) = \epsilon_1(1-\epsilon_2)\frac{2n}{\eta}\;\frac{[I_nK_n'+K_nI_n']I_n(k\eta)}{1-\epsilon_1 k(I_nK_n'+K_nI_n')}\;, \tag{25a}$$

$$T_n^{(j)}(k,\eta) = \epsilon_1\frac{2n}{\eta k}\left\{\frac{2kK_nK_n'I_n(k\eta)}{1-\epsilon_1 k(I_nK_n' + K_nI_n')} + K_n\left(\frac{k}{\eta}\right)\right\}. \tag{25b}$$

In (25) those Bessel functions whose arguments are omitted have the argument k.

For a whole vortex line of distribution $\Gamma(y)$ ranging from $y = -b_1$ to b_2 and extending through a jet, the solution of φ_2 is obtained immediately by integrating the Green's functions of part (1) and (2). This expression, however, will not be explicitly written down here, but will be included in the final form of the total perturbation potential given as follows. In summary,

$$\varphi(x,y,z) = \varphi_1(y,z) + \varphi_2(x,y,z) \tag{26a}$$

and with the notation $\varphi = \varphi_o$ for $r > 1$ and $\varphi = \varphi_j$ for $r < 1$, then

$$\begin{aligned} 4\pi\varphi_o = &\int_{-b_1}^{b_2}\Gamma(\eta)F(x,y-\eta,z)d\eta - \epsilon_2\int_{-1}^{1}\Gamma(\eta)F(x,y-\eta,z)d\eta \\ &+\epsilon_1\left(\int_{-b_1}^{-1}+\int_1^{b_2}\right)\frac{\Gamma(\eta)}{\eta^2}\,F\left(x,y-\frac{1}{\eta},z\right)d\eta \\ &+\frac{2}{\pi}\sum_{n=1}^{\infty}\sin n\theta\int_0^{\infty}K_n(kr)\sin kx\,dk\left[\int_{-b_1}^{-1}+\int_1^{b_2}\Gamma(\eta)S_n^{(o)}(k,\eta)d\eta\right. \\ &\left.+\int_{-1}^{1}\Gamma(\eta)T_n^{(o)}(k,\eta)\,d\eta\right]\;, \end{aligned} \tag{26b}$$

$$4\pi\varphi_j = \int_{-b_1}^{b_2} \Gamma(\eta)F(x, y-\eta, z)d\eta - \epsilon_2\left(\int_{-b_1}^{-1} + \int_{1}^{b_2}\right)\Gamma(\eta)F(x, y-\eta, z)d\eta$$

$$- \epsilon_1\int_{-1}^{1} \frac{\Gamma(\eta)}{\eta^2} F(x, y-\frac{1}{\eta}, z)d\eta + \frac{2}{\pi}\sum_{n=1}^{\infty} \sin n\theta \int_0^{\infty} I_n(kr)\sin kx\, dk\left[\int_{-b}^{-1}\right.$$

$$\left. + \int_1^{b_2} \Gamma(\eta)S_n^{(j)}(k, \eta)d\eta + \int_{-1}^{1} \Gamma(\eta)T_n^{(j)}(k, \eta)d\eta\right], \qquad (26c)$$

where

$$F(x, y, z) = F_1(y, z) + F_2(x, y, z) = \frac{z}{y^2+z^2}\left[1 + \frac{x}{(x^2+y^2+z^2)^{1/2}}\right]. \qquad (26d)$$

By using the rule (21), it may be noted from (22) and (25) that

$$S_n^{(o, j)}(k, -\eta) = (-)^{n+1}S_n^{(o, j)}(k, \eta), \qquad T_n^{(o, j)}(k, -\eta) = (-)^{n+1}T_n^{(o, j)}(k, \eta).$$

Hence, if $b_1 = b_2$ and if $\Gamma(-\eta) = \Gamma(\eta)$, then the even terms in the infinite series all cancel out; similarly, the odd terms vanish if $\Gamma(-\eta) = -\Gamma(\eta)$. It therefore follows that, with $b_1 = b_2$,

$$\varphi(x, -y, z) = \pm\, \varphi(x, y, z) \quad \text{for} \quad \Gamma(-\eta) = \pm\, \Gamma(\eta).$$

As $V_j \to V_o$, or $\mu \to 1$, we have $\epsilon_1, \epsilon_2 \to 0$ (see Eq. 7), then only the first term on the right side of (26b, c) remains, which is known to be the lifting line potential in an otherwise uniform flow. On the other hand, if $V_o = 0$, $V_j > 0$, then $\epsilon_1 = \epsilon_2 = 1$; thus (26) reduces to the potential of a lifting line extending through a free jet, that is, for $r < 1$,

$$\varphi = \frac{1}{4\pi}\int_{-1}^{1} \Gamma(\eta)\,\{F(x, y-\eta, z) - \frac{1}{\eta^2}\, F(x, y-\frac{1}{\eta}, z)\}d\eta$$

$$+ \frac{1}{\pi^2}\sum_{n=1}^{\infty} n \sin n\theta \int_0^{\infty} I_n(kr)\,\frac{\sin kx}{k}\, dk$$

$$\times \int_{-1}^{1} \left\{ \frac{2kK_nK_n'I_n(k\eta)}{i-k(I_nK_n'+K_nI_n')} + K_n(\frac{k}{\eta}) \right\} \frac{\Gamma(\eta)}{\eta}\, d\eta\,. \tag{27}$$

The solution φ_o for $r > 1$ of course loses its meaning. In the general case the terms with the factors ϵ_1 and ϵ_2 represent the effect of the jet on the potential φ.

2. The Fourier Expansion for Circulation; Lift Distribution

The spanwise lift distribution, $\ell(y)$, defined to be the local lift on a unit span of the wing at station y, is given by the Joukowsky theorem

$$\ell(y) = \rho V_{local}\Gamma(y), \tag{28}$$

where $V_{local} = V_o$ for $r > 1$ and $= V_j$ for $r < 1$. The total lift on the wing is then

$$L = \int_{span} \ell(y)\, dy = \rho\int_{span} V_{local}\Gamma(y)\, dy\,. \tag{29}$$

At the boundary of the jet $(y = \pm 1)$, the lift distribution must be continuous. Hence it follows from (28) that the conditions

$$\Gamma(1-0) = \mu\Gamma(1+0) \quad \text{and} \quad \Gamma(-1+0) = \mu\Gamma(-1-0) \tag{30}$$

must be satisfied. These conditions show that the circulation Γ will have a jump at the jet boundary. It should be pointed out here that the continuity of the wing surface at the jet boundary requires further that the downwash be continuous at the boundary; this condition remains to be enforced, (see Equations 45, 46).

In the following sections dealing with the single jet problem, we shall limit ourselves to the case $b_1 = b_2 = b$, i.e., a single jet centered at the mid-span. It is convenient to divide the span into two regions:

$$R_o: \quad 1 < |y| < b \quad \text{and} \quad R_1: \quad |y| < 1,$$

and define the angles ψ_o, ψ_1 (see Fig. 2) by

$$y = b \cos \psi_o \qquad \text{for } 1 < |y| < b, \tag{31a}$$

$$y = b \cos \psi_o = \cos \psi_1 \qquad \text{for } |y| < 1, \tag{31b}$$

so that

$$\psi_o = \cos^{-1}\frac{1}{b} \equiv \beta \qquad \text{and} \quad \psi_1 = 0 \quad \text{at} \quad y = 1. \tag{31c}$$

In order to account for the possible slipstream rotation of small magnitude, the circulation $\Gamma(y)$ is not to be limited to even functions of y. We now assume that $\Gamma(y)$ can be represented by the following Fourier series:

$$\Gamma(y) = 4V_j\Gamma_\nu(y) \quad \text{in region } R_\nu, \quad \nu = 0, 1, \tag{32a}$$

$$\Gamma_o(y) = \sum_{n=1}^{2N_o} A_n^{(0)} \sin n\psi_o \quad \text{in } R_o, \tag{32b}$$

$$\Gamma_1(y) = \Gamma_o(y) + A_o^{(1)} + \sum_{n=1}^{2N_1} A_n^{(1)} \sin n\psi_1 \quad \text{in } R_1 \tag{32c}$$

in which the numbers N_o and N_1 may be set as large as we wish, or as practical. The expansion for $\Gamma_o(y)$ is suggested by the usual lifting line theory. In (32c) the constant $A_o^{(1)}$ is introduced in order to satisfy the jump conditions (30), the difference between $\Gamma_1(y)$ and $\Gamma_o(y) + A_o^{(1)}$ in $|y| < 1$ is chosen to be a sine series since first, the half-period Fourier expansion in $0 < \psi_1 < \pi$ is rather arbitrary and second, the sine series is more amenable to analysis than the cosine expansion. Now application of condition (30) to (32) yields

$$A_o^{(1)} = (\mu - 1) \sum_{n=0}^{N_o - 1} A_{2n+1}^{(0)} \sin (2n+1)\beta, \tag{33a}$$

$$0 = \sum_{n=0}^{N_o} A_{2n}^{(0)} \sin 2n\beta \, . \tag{33b}$$

If there is no slipstream rotation and if the angle of attack is symmetric about the mid-span, then $A_{2n}^{(0)} = A_{2n}^{(1)} = 0$ and hence (33b) is automatically fulfilled.

Substituting (32) into (29) and integrating, we obtain

$$\frac{L}{8\rho V_j^2} = A_o^{(1)} + \frac{\pi}{4}(bA_1^{(0)} + A_1^{(1)})$$
$$+ (\mu-1)b \sum_{n=0}^{N_o - 1} A_{2n+1}^{(0)} \left[\frac{\sin 2n\beta}{4n} - \frac{\sin 2(n+1)\beta}{4(n+1)} \right] \tag{34}$$

It is noted here that the terms with $A_n^{(1)}$ for $n > 1$ and $A_{2n}^{(0)}$ make no contribution to the total lift.

3. Downwash Distribution

According to the approximate lifting surface theory of Weissinger[8], the wing and its wake are represented by a bound vortex line located at the quarter chord (which is also the center of pressure) together with a system of trailing vortices as in the lifting line theory, and the flow is then required to be tangential to the wing surface at the three-quarter chord points. Let the quarter chord be located at $x = 0$ and let $c(y)$ be the half-chord length at y, then the downwash at the three-quarter chord is

$$w(y) = -\partial\varphi(c, y, 0)/\partial z \; . \tag{35}$$

In carrying out the differentiation we note from (26d) that

$$F_z(c, y-\eta, 0) = \frac{1}{(y-\eta)^2}\left\{1 + \frac{c}{[(y-\eta)^2+c^2]^{1/2}}\right\} = \frac{\partial}{\partial\eta}\, G(y-\eta, c), \tag{36a}$$

$$\frac{1}{\eta^2}\, F_z(c, y-\frac{1}{\eta}, 0) = \frac{1}{\eta^2}\, \frac{\partial}{\partial(1/\eta)}\, G(y-\frac{1}{\eta}, c) = -\frac{\partial}{\partial\eta}\, G(y-\frac{1}{\eta}, c)\,, \tag{36b}$$

where

$$G(y, c) = G_1(y) + G_2(y, c), \tag{37a}$$

$$G_1(y) = \frac{2}{y}, \quad G_2(y, c) = \frac{1}{y}\left[\left(1+\frac{y^2}{c^2}\right)^{1/2} - 1\right] = \frac{y}{c^2}\Big/\left[1+\left(1+\frac{y^2}{c^2}\right)^{1/2}\right]. \tag{37b}$$

The function $G(y, c)$ is decomposed as shown above such that $G_2(y, c)$ is regular for all y and for $c > 0$, the only singular part of G being $G_1(y)$. It can be seen that $G_1(y)$ actually corresponds to the value of G at large distances behind the wing (the so-called Treffetz plane solution).

By using (36), the integrals containing F_z in the expression for w can be integrated once by parts. Doing so, we find that the terms evaluated at the limits $y = \pm 1$ and $y = -b, b$ all vanish on account of condition (30), relations (7a), and the condition that $\Gamma(-b) = \Gamma(b) = 0$. Furthermore,

$$\frac{\partial}{\partial z}[K_n(kr)\sin n\theta]_{z=0} = \frac{1}{y}\frac{\partial}{\partial\theta}[K_n(kr)\sin n\theta]_{z=0} = \frac{n}{y}K_n(ky)$$

which is valid for both $y > 0$ $(\theta = 0)$ and $y < 0$ $(\theta = \pi)$ provided the continuation of $K_n(kr)$ from $\theta = 0$ to $\theta = \pi$ follows the rule (21). The same result applies if K_n is replaced by I_n. In summary, we obtain the downwash $w(y) = w_o(y)$ for $1 < |y| < b$ and $w(y) = w_j(y)$ for $|y| < 1$, as follows

$$\begin{aligned}4\pi w_o(y) = {} & \int_{-b}^{b} G(y-\eta, c)\frac{d\Gamma}{d\eta}d\eta - \epsilon_2\int_{-1}^{1} G(y-\eta, c)\frac{d\Gamma}{d\eta}d\eta \\ & - \epsilon_1\left(\int_{-b}^{1} + \int_{1}^{b}\right)G(y-\frac{1}{\eta}, c)\frac{d\Gamma}{d\eta}d\eta \\ & - \frac{2}{\pi}\sum_{\nu=1}^{\infty}\frac{\nu}{y}\int_0^{\infty}K_\nu(ky)\sin kc\, dk\left[\int_{-b}^{-1} + \int_1^b S_\nu^{(o)}(k, \eta)\Gamma(\eta)d\eta\right. \\ & \left. + \int_{-1}^{1}T_\nu^{(o)}(k, \eta)\Gamma(\eta)\,d\eta\right], \end{aligned} \tag{38a}$$

$$\begin{aligned}4\pi w_j(y) = {} & \int_{-b}^{b} G(y-\eta, c)\frac{d\Gamma}{d\eta}d\eta - \epsilon_2\left(\int_{-b}^{-1} + \int_{1}^{b}\right)G(y-\eta, c)\frac{d\Gamma}{d\eta}d\eta \\ & + \epsilon_1\int_{-1}^{1} G(y-\frac{1}{\eta}, c)\frac{d\Gamma}{d\eta}d\eta - \frac{2}{\pi}\sum_{\nu=1}^{\infty}\frac{\nu}{y}\int_0^{\infty}I_\nu(ky)\sin kc\, dk\left[\int_{-b}^{-1}\right. \\ & \left. + \int_1^b S_\nu^{(j)}(k, \eta)\Gamma(\eta)d\eta + \int_{-1}^{1}T_\nu^{(j)}(k, \eta)\Gamma(\eta)d\eta\right]. \end{aligned} \tag{38b}$$

Now we substitute the series expansion for Γ given by (32) into (38), we note that some of the resulting integrals can be evaluated in closed form. For example,

$$P\int_0^{\pi} \frac{\cos n\theta \, d\theta}{\cos\theta - \cos\psi} = \pi \frac{\sin n\psi}{\sin\psi},$$

$$\int_0^{\pi} \frac{\cos n\theta \, d\theta}{\cos\theta - y} = -(\operatorname{sgn} y)^{n+1}\pi[\,|y| - (y^2-1)^{1/2}]^n/(y^2-1)^{1/2}, \quad \text{for } |y| > 1,$$

where P denotes the Cauchy principal value of the integral, and $(y^2-1)^{1/2}$ represents the positive branch of that function. After some rearrangement we obtain the following expression for the downwash $w(y)$:

a. <u>for $1 < |y| < b$</u>

$$\frac{w_o}{V_j} = \sum_{n=1}^{2N_o} \frac{n}{b} A_n^{(0)} \Big\{ 2\frac{\sin n\psi_o}{\sin\psi_o} + \Omega_n(\tfrac{y}{b};\tfrac{b}{c};R_o+R_1) - \epsilon_2[P_n(\tfrac{y}{b};R_1) + \Omega_n(\tfrac{y}{b},\tfrac{b}{c};R_1)]$$

$$-\epsilon_1 b^2[Q_n(by;R_o) + \Lambda_n(by;\tfrac{1}{bc};R_o)]\Big\}$$

$$+(1-\epsilon_2)\sum_{n=1}^{2N_1} nA_n^{(1)} \Big\{ -2(\operatorname{sgn} y)^{n+1} \frac{[\,|y| - (y^2-1)^{1/2}]^n}{(y^2-1)^{1/2}} + \Omega_n(y;\tfrac{1}{c};R_o+R_1)\Big\}$$

$$-\frac{2}{\pi^2}\sum_{\nu=1}^{\infty} \frac{\nu}{y}\int_0^{\infty} K_\nu(ky)\sin kc\,dk \Big\{ \Big(\int_{-b}^{-1} + \int_1^b\Big) S_\nu^{(0)}(k,\eta)\Gamma_o(\eta)d\eta + \int_{-1}^{1} T_\nu^{(0)}(k,\eta)\Gamma_1(\eta)d\eta \Big\}; \tag{39a}$$

b. <u>for $|y| < 1$</u>

$$\frac{w_j}{V_j} = \sum_{n=1}^{2N_o} \frac{n}{b} A_n^{(0)} \Big\{ 2\frac{\sin n\psi_o}{\sin\psi_o} + \Omega_n(\tfrac{y}{b};\tfrac{b}{c};R_o+R_1) - \epsilon_2[P_n(\tfrac{y}{b};R_o) + \Omega_n(\tfrac{y}{b},\tfrac{b}{c};R_o)]$$

$$+\epsilon_1 b^2[Q_n(by;R_1) + \Lambda_n(by;\tfrac{1}{bc};R_1)]\Big\}$$

$$+\sum_{n=1}^{2N_1} nA_n^{(1)} \Big\{ 2\frac{\sin n\psi_1}{\sin\psi_1} + \Omega_n(y;\tfrac{1}{c};R_o+R_1) + \epsilon_1\Big[\frac{2}{(1-y^2)^{1/2}} \frac{y^{n-1}}{[1+(1-y^2)^{1/2}]^n}$$

$$+ \Lambda_n(y;\tfrac{1}{c};R_o+R_1)\Big]\Big]\Big\} - \frac{2}{\pi^2}\sum_{\nu=1}^{\infty}\frac{\nu}{y}\int_0^{\infty} I_\nu(ky)\sin kc\,dk\left\{\int_{-b}^{-1}\right.$$

$$\left. + \int_1^b S_\nu^{(j)}(k,\eta)\,\Gamma_o(\eta)d\eta + \int_{-1}^{1} T_\nu^{(j)}(k,\eta)\Gamma_1(\eta)\,d\eta\right\} . \qquad (39b)$$

In the above equations the new functions P_n, Q_n, Ω_n and Λ_n are defined as follows:

$$P_n(\zeta;R_o) = \frac{2}{\pi}\int_0^{\beta} + \int_{\pi-\beta}^{\pi} \frac{\cos n\theta\, d\theta}{\cos\theta - \zeta} , \qquad (40a)$$

$$P_n(\zeta;R_1) = \frac{2}{\pi}\int_{\beta}^{\pi-\beta} \frac{\cos n\theta\, d\theta}{\cos\theta - \zeta} , \qquad (40b)$$

$$Q_n(\zeta;R_o) = \frac{2}{\pi}\int_0^{\beta} + \int_{\pi-\beta}^{\pi} \frac{\cos\theta\cos n\theta}{1-\zeta\cos\theta}\, d\theta , \qquad (41a)$$

$$Q_n(\zeta;R_1) = \frac{2}{\pi}\int_{\beta}^{\pi-\beta} \frac{\cos\theta\cos n\theta}{1-\zeta\cos\theta}\, d\theta , \qquad (41b)$$

$$\Omega_n(\zeta;\lambda;R_o) = \int_0^{\beta} f_n(\zeta;\lambda;\theta)d\theta, \quad \Omega_n(\zeta;\lambda;R_1) = \int_{\beta}^{\pi/2} f_n(\zeta;\lambda;\theta)d\theta , \qquad (42a)$$

$$f_n(\zeta;\lambda;\theta) = \frac{\lambda^2}{\pi}\left\{\frac{(\cos\theta-\zeta)\cos n\theta}{1+[1+\lambda^2(\cos\theta-\zeta)^2]^{1/2}} + \frac{(-)^{n+1}(\cos\theta+\zeta)\cos n\theta}{1+[1+\lambda^2(\cos\theta+\zeta)^2]^{1/2}}\right\}. \qquad (42b)$$

$$\Omega_n(\zeta;\lambda;R_o+R_1) = \Omega_n(\zeta;\lambda;R_o) + \Omega_n(\zeta;\lambda;R_1).$$

$$\Lambda_n(\zeta;\lambda;R_o) = \int_0^{\beta} g_n(\zeta;\lambda;\theta)d\theta, \quad \Lambda_n(\zeta;\lambda;R_1) = \int_{\beta}^{\pi/2} g_n(\zeta;\lambda;\theta)d\theta , \qquad (43a)$$

$$g_n(\zeta;\lambda;\theta) = \frac{\lambda^2}{\pi}\left\{\frac{(\sec\theta-\zeta)\cos n\theta}{1+[1+\lambda^2(\sec\theta-\zeta)^2]^{1/2}} + (-)^{n+1}\frac{(\sec\theta+\zeta)\cos n\theta}{1+[1+\lambda^2(\sec\theta+\zeta)^2]^{1/2}}\right\},$$

(43b)

$$\Lambda_n(\zeta;\lambda;R_o+R_1) = \Lambda_n(\zeta;\lambda;R_o) + \Lambda_n(\zeta;\lambda;R_1).$$

The functions $\Omega_n(\zeta,\lambda)$ and $\Lambda_n(\zeta,\lambda)$ are readily seen to be regular functions for finite ζ and λ (that is, for $c > 0$). The functions P_1 and Q_1 defined by the above integral representation can be integrated in closed form, and P_n, Q_n (for $n > 1$) can be expressed in terms of elementary functions and P_1 and Q_1. For the purpose of numerical computation, however, it is quite convenient to apply the modified Simpson's rule directly to evaluate these integrals. For large values of n, the most significant contribution from the integrand comes from the neighborhood of the points of stationary phase. As to the analytic behavior of P_n and Q_n, it is noted that they all have a logarithmic similarity at the jet boundary $y = \pm 1$. In fact, it can be shown that if ϵ is a small positive quantity, then for $y = 1 + \epsilon$,

$$P_n\left(\frac{y}{b};R_1\right) \cong + \frac{\cos n\beta}{\pi \sin \beta} \log \epsilon + O(1), \quad Q_n(by;R_o) \cong \frac{\cos n\beta}{\pi b^2 \sin \beta} \log \epsilon + O(1) \;; \tag{44a}$$

and for $y = 1 - \epsilon$,

$$P_n\left(\frac{y}{b};R_o\right) \cong - \frac{\cos n\beta}{\pi \sin \beta} \log \epsilon + O(1) \,, \quad Q_n(by;R_1) \cong - \frac{\cos n\beta}{\pi b^2 \sin \beta} \log \epsilon + O(1) \,. \tag{44b}$$

The singular behavior of these functions at $y = -1$ can be deduced from the above results by using the relations

$$P_n(-\zeta;R) = (-)^{n+1} P_n(\zeta;R) \,, \qquad Q_n(-\zeta;R) = (-)^{n+1} Q_n(\zeta;R) \,. \tag{44c}$$

Aside from the logarithmic singularities of P_n and Q_n, we further note from (39) that the downwash $w(y)$ also has square root singularities at the jet boundary, which are proportional to $(y^2-1)^{-1/2}$ or $(1-y^2)^{-1/2}$ as they appear in the series $\sum nA_n^{(1)}$. The strengths of these square root singularities are seen to be independent of both the span b and chord c, whereas the strengths of the logarithmic singularities (see Eq. 44) depend on b, but not on c. This implies that all these singularities are solely due to the effect of the slipstream boundary, and therefore are inherent in both the lifting line and lifting surface theory.

Now we must ensure that the downwash does not become infinite at the slipstream boundary if the wing surface is continuous there. In order that the square root singularities of $w(y)$ at $y = 1$ and $y = -1$ shall be eliminated, the relations

$$\sum_{n=0}^{N_1-1} (2n+1)A_{2n+1}^{(1)} = 0 \tag{45a}$$

and

$$\sum_{n=1}^{N_1} 2nA_{2n}^{(1)} = 0 \tag{45b}$$

must therefore be satisfied. Furthermore, in order to remove the logarithmic singularities of $w(y)$ at $y = \pm 1$, the additional relations

$$\sum_{n=0}^{N_o-1} (2n+1)A_{2n+1}^{(0)} \cos (2n+1)\beta = 0 \tag{46a}$$

and

$$\sum_{n=1}^{N_o} 2nA_{2n}^{(0)} \cos 2n\beta = 0 \tag{46b}$$

must also be satisfied. Conditions (45a, b) and (46a, b) may be regarded as four constraints on the coefficients $A_n^{(0)}$ and $A_n^{(1)}$ so that the downwash will be finite at the jet boundary.

It is convenient for the purpose of numerical computation to first remove the singularities in the expressions for w_o and w_j by applying the conditions (45), (46), or, which is equivalent, by making in (39a, b) the following replacements:

$$-2(\operatorname{sgn} y)^{n+1}\frac{[|y|-(y^2-1)^{1/2}]^n}{(y^2-1)^{1/2}} \quad \text{by} \quad 2(\operatorname{sgn} y)^{n+1}\frac{1-[|y|-(y^2-1)^{1/2}]^n}{(y^2-1)^{1/2}} ,$$

$$\frac{2}{(1-y^2)^{1/2}}\frac{y^{n-1}}{[1+(1-y^2)^{1/2}]^n} \quad \text{by} \quad \frac{2}{(1-y^2)^{1/2}}\left\{\frac{y^{n-1}}{[1+(1-y^2)^{1/2}]^n} - (\operatorname{sgn} y)^{n-1}\right\},$$

$$P_n(\tfrac{y}{b};R_o) \quad \text{by} \quad P_n^*(\tfrac{y}{b};R_o) = \frac{2}{\pi}\int_0^{\beta}\left[\frac{1}{\cos\theta-\frac{y}{b}}+\frac{(-1)^{n+1}}{\cos\theta+\frac{y}{b}}\right](\cos n\theta-\cos n\beta)d\theta ,$$

$$P_n(\tfrac{y}{b};R_1) \quad \text{by} \quad P_n^*(\tfrac{y}{b};R_1) = \frac{2}{\pi}\int_{\beta}^{\pi/2}\left[\frac{1}{\cos\theta-\frac{y}{b}}+\frac{(-1)^{n+1}}{\cos\theta+\frac{y}{b}}\right](\cos n\theta-\cos n\beta)d\theta ,$$

$$Q_n(by;R_o) \quad \text{by} \quad Q_n^*(by;R_o) = \frac{2}{\pi}\int_0^{\beta}\left[\frac{\cos\theta}{1-by\cos\theta}+\frac{(-)^{n+1}\cos\theta}{1+by\cos\theta}\right](\cos n\theta-\cos n\beta)d\theta ,$$

$$Q_n(by;R_1) \quad \text{by} \quad Q_n^*(by;R_1) = \frac{2}{\pi}\int_{\beta}^{\pi/2}\left[\frac{\cos\theta}{1-by\cos\theta}+\frac{(-)^{n+1}\cos\theta}{1+by\cos\theta}\right](\cos n\theta-\cos n\beta)d\theta .$$

With these substitutions the downwash $w(y)$ is therefore regular everywhere over the wing. Although conditions (45a, b) and (46a, b) have been once applied as shown in the above substitutions, they must still be used in the calculation of the coefficients $A_n^{(0)}$ and $A_n^{(1)}$ since no coefficient is actually eliminated in this process.

4. Application of Boundary Conditions on the Wing

In order to take the effect of small slipstream rotation into account, we make the following simplifying assumptions.

1. The axis of the cylindrical slipstream is parallel to the undisturbed main stream and passes through the mid-chord point of the wing. The velocity of the slipstream may have a rotational component with distribution $r\omega(r)$ about the jet axis, where

r is the radial distance and ω is the angular velocity, ω being taken positive if the rotation is counterclockwise when viewed from the rear. The rotation is assumed to be small, that is, $|\omega|_{max}/V_j << 1$ for $r \leq 1$.

2. The effect of rotation is equivalent to a change in the stream direction at the wing, giving rise to a variation in the effective wing incidence inside the slipstream, but is assumed to have no effect outside the jet.

3. The rotational velocity of the slipstream does not vary appreciably in the region over the wing.

Hence, if $\alpha(y)$ denotes the local geometric angle of attack at station y of the 3/4 chord line, then the boundary condition that $w(y)/V_{local}$ is equal to the local effective angle of attack may be written

$$w_j(y)/V_j = \alpha(y) + y\omega(y)/V_j \qquad \text{for } |y| < 1, \tag{47a}$$

$$w_o(y)/V_o = \alpha(y) \qquad \text{for } 1 < |y| < b\ . \tag{47b}$$

Obviously $\omega(-y) = \omega(y)$ so that $y\omega(y)$ is an odd function of y. However, in general practice the geometric wing incidence is symmetric about the central span so that

$$\alpha(-y) = \alpha(y) \qquad \text{for } |y| < b\ . \tag{48}$$

Since in the conditions (45a, b) and (46a, b) the odd and even terms are not coupled, it becomes convenient to decompose the problem into even and odd parts as follows.

a. The Even Part

The boundary conditions of this part reads

$$w_{j,\,even}(y)/V_j = \alpha(y) \qquad \text{for} \quad 0 < y < 1 \tag{49a}$$

$$w_{o,\,even}(y)/V_o = \alpha(y) \qquad \text{for} \quad 1 < y < b \tag{49b}$$

where $w_{j,\,even}$ and $w_{o,\,even}$ are respectively the even part of w_j and w_o, which can be obtained directly from (39) by deleting the even terms with $n = 2, 4, 6, \ldots, 2N$. The two conditions (49a, b) contain $N_o + N_1$ unknown coefficients $A^{(0)}_{2n+1}$, $A^{(1)}_{2n+1}$, which should be determined under the constraints (45a) and (46a). Hence we may take $(N_o + N_1 - 2)$ appropriate points in $0 < y < b$ at which we apply conditions (49a, b). For instance, we may choose (N_1-1) points in $0 < y < 1$ and (N_o-1) points in $1 < y < b$.

b. The Odd Part

For this part we have the boundary conditions

$$w_{j,\,odd}(y) = y\omega(y) \qquad \text{for} \quad 0 < y < 1\,, \tag{50a}$$

$$w_{o,\,odd}(y) = 0 \qquad \text{for} \quad 1 < y < b\,, \tag{50b}$$

where $w_{j,\,odd}$ and $w_{o,\,odd}$ are the odd part of w_j and w_o, which are obtained from (39) by deleting the odd terms with $n = 1, 3, 5, \ldots$. These two conditions contain $(N_o + N_1)$ unknown coefficients $A^{(0)}_{2n}$ and $A^{(1)}_{2n}$, which must also satisfy conditions (45b) and (46b). The same points chosen for the even part may also be used for this part. Thus the problem is now reduced to solving a system of $(N_o + N_1)$ linear algebraic equations in either the even or odd part.

C. MULTIPLE JET THEORY

1. Geometric Configuration of a Wing and Multiple Jet System

We suppose that there are in general J pairs of jet slipstreams which are symmetrically located with respect to the mid-span, so that the total number of jets is $2J$. All the slipstreams are assumed to be circular cylinders, with their central axes parallel to the main stream and passing through the center-chord points of the wing. The span of the wing is divided into $(2J + 1)$ regions, denoted by R_ν, $\nu = 0, 1, 2, \ldots, 2J$, which are defined as follows (see Fig. 3).

R_o is the region on the span outboard of all the jets;

$R_{2\nu-1}$ is the region inside the νth jet pair, $\nu = 1, 2, \ldots, J$, counted from the wing tip toward the center;

$R_{2\nu}$ is the region between the νth and the $(\nu+1)$th jet pairs.

The boundaries of these regions along the y-axis are marked by the points

$$-b_o = -b, -b_1, -b_2, \ldots, -b_{2J}, \quad b_{2J+1} = 0, \quad b_{2J}, \ldots, b_2, b_1, b_o = b.$$

For every point y in the region R_ν we define $(\nu+1)$ angles, denoted by ψ_s, by

$$y = b_s \cos \psi_s, \quad s = 0, 1, 2, \ldots, \nu, \quad \text{for } b_{\nu+1} < |y| \leq b_\nu \; . \qquad (51)$$

At the point $y = b_\nu$, let

$$\psi_s = \beta_s^{(\nu)} = \cos^{-1}(b_\nu/b_s), \quad s = 0, 1, 2, \ldots, \nu, \quad \nu = 0, 1, \ldots, 2J \; . \qquad (52)$$

Furthermore, all the jets are assumed to have the same radius, which is normalized to unity. The centers of the νth jet pair are at $y = a_\nu$

and $y = -a_\nu$, where

$$a_\nu = \frac{1}{2}(b_{2\nu-1} + b_{2\nu}), \quad a_{-\nu} = -a_\nu, \quad \nu = 1, 2, \ldots, J. \qquad (53)$$

Finally, the geometric incidence of the wing and the slipstream rotation of the jet pairs, if any, are both assumed to be small and symmetric about the mid-span.

2. Velocity Potential of a Wing Extending through Multiple Jets

The image system of a vortex element due to a single slipstream has been determined in Section B1; it will be called the primary image system for the problem of multiple jet slipstreams. The image system of a vortex element generated by a set of multiple jets contains the images of the primary and higher orders (i. e. the images of the primary system and in turn their images) since it takes the images of infinite orders to completely satisfy conditions (4) and (5) at all the slipstream boundaries. In order to simplify the analysis, the image system of a vortex element due to a set of jets will be determined by taking into account only the primary and secondary images and by neglecting the images of higher orders. The final result of this approximation is expected to be accurate enough for practical applications. In this manner the two-dimensional part of the velocity potential can be obtained as follows.

a. For a Vortex Element $\Gamma(\eta)\delta\eta$ located at $y = \eta$ in $R_{2\nu}$ (Outside All the Jets)

φ_o outside all the jets is due to $\Gamma(\eta)\delta\eta$ at $y = \eta$ plus $\frac{\epsilon_1}{(\eta-a_\ell)^2}\Gamma(\eta)\delta\eta$ at $y = a_\ell + \frac{1}{\eta-a_\ell}$, summing over ℓ, $\ell = -J, \ldots J$;

$\varphi_{j,\lambda}$ inside the λth jet is due to $(1-\epsilon_2)\Gamma(\eta)\delta\eta$ at $y = \eta$ plus $\frac{\epsilon_1(1-\epsilon_2)}{(\eta-a_\ell)^2}\Gamma(\eta)\delta\eta$ at $y = a_\ell + \frac{1}{\eta-a_\ell}$, summing over ℓ, $\neq \lambda$.

b. For a Vortex Element $\Gamma(\eta)\delta\eta$ located at $y = \eta$ Inside the λth Jet

φ_0 outside all the jets is due to $(1-\epsilon_2)\Gamma(\eta)\delta\eta$ at $y = \eta$ plus $\frac{\epsilon_1(1-\epsilon_2)}{(\eta-a_\ell)^2}\Gamma(\eta)\delta\eta$ at $y = a_\ell + \frac{1}{\eta-a_\ell}$, summing over ℓ, $\neq \lambda$;

$\varphi_{j,\ell}$ in the ℓth jet is due to $(1-\epsilon_2)^2\Gamma(\eta)\delta\eta$ at $y = \eta$, for ℓ, $\neq \lambda$;

$\varphi_{j,\lambda}$ in the λth jet is due to $\Gamma(\eta)\delta\eta$ at $y = \eta$, plus $-\frac{\epsilon_1}{(\eta-a_\lambda)^2}\Gamma(\eta)\delta\eta$ at $y = a_\lambda + \frac{1}{\eta-a_\lambda}$, plus $\frac{\epsilon_1(1-\epsilon_2)^2}{(\eta-a_\ell)^2}\Gamma(\eta)\delta\eta$ at $y = a_\ell + \frac{1}{\eta-a_\ell}$, summing over ℓ, $\neq \lambda$.

Again, like the previous case of a single jet, the three-dimensional part of the potential can be decomposed into two components, of which one part can be written down according to the same image system as given above, and the rest can be expanded in a Fourier-Bessel series. Since it has been found that the contribution of the Fourier-Bessel series is very small, this part of the velocity potential will be constructed by including only the images in the immediate neighboring regions, whereas the images in the other regions and the higher order images will be neglected. Thus, summing up all the vortex elements along the span, we obtain the following result for φ. With $\varphi = \varphi_0$ outside all the jets and $\varphi = \varphi_{j,\lambda}$ inside the λth jet (which will be taken to be one on the positive y-axis), we have

$$4\pi\varphi_o = \sum_{\nu=0}^{J}\int_{-b_{2\nu}}^{-b_{2\nu+1}} + \int_{b_{2\nu+1}}^{b_{2\nu}} \left\{ F(x, y-\eta, z) + \sum_{\ell=-J}^{J} \frac{\epsilon_1}{(\eta-a_\ell)^2} F(x, y-a_\ell - \frac{1}{\eta-a_\ell}, z) \right\} \Gamma(\eta) d\eta$$

$$+ (1-\epsilon_2) \sum_{\nu=1}^{J} \int_{-b_{2\nu-1}}^{-b_{2\nu}} + \int_{b_{2\nu}}^{b_{2\nu-1}} \left\{ F(x, y-\eta, z) + \sum_{\ell=-J}^{J}{}'' \frac{\epsilon_1}{(n-a_\ell)^2} F(x, y-a_\ell - \frac{1}{\eta-a_\ell}, z) \right\} \Gamma(\eta) d\eta$$

$$+ \frac{2}{\pi} \sum_{\ell=-J}^{J} \sum_{m=1}^{\infty} \sin m\theta_\ell \int_0^\infty K_m(kr_\ell) \sin kx \, dk \left\{ \int_{b_{2\ell+1}}^{b_{2\ell}} + \int_{b_{2\ell-1}}^{b_{2\ell-2}} S_m^{(o)}(k, \eta-a_\ell)\Gamma(\eta) d\eta \right.$$

$$\left. + \int_{b_{2\ell}}^{b_{2\ell-1}} T_m^{(o)}(k, \eta-a_\ell)\Gamma(\eta) d\eta \right\} , \tag{54a}$$

$$4\pi\varphi_{j,\lambda} = (1-\epsilon_2) \sum_{\nu=0}^{J} \int_{-b_{2\nu}}^{-b_{2\nu+1}} + \int_{b_{2\nu+1}}^{b_{2\nu}} \left\{ F(x, y-\eta, z) \right.$$

$$\left. + \sum_{\substack{\ell=-J \\ (\ell\neq\lambda)}}^{J}{}' \frac{\epsilon_1}{(\eta-a_\ell)^2} F(x, y-a_\ell - \frac{1}{\eta-a_\ell}, z) \right\} \Gamma(\eta) d\eta + \int_{b_{2\lambda}}^{b_{2\lambda-1}} F(x, y-\eta, z)\Gamma(\eta) d\eta$$

$$+ (1-\epsilon_2)^2 \left\{ \sum_{\substack{\nu=1 \\ (\nu\neq\lambda)}}^{J}{}' \int_{b_{2\nu}}^{b_{2\nu-1}} F(x, y-\eta, z)\Gamma d\eta + \sum_{\nu=1}^{J} \int_{-b_{2\nu-1}}^{-b_{2\nu}} F(x, y-\eta, z)\Gamma d\eta \right\}$$

$$- \int_{b_{2\lambda}}^{b_{2\lambda-1}} \left\{ \frac{\epsilon_1}{(\eta-a_\lambda)^2} F(x, y-a_\lambda - \frac{1}{\eta-a_\lambda}, z) - \sum_{\substack{\ell=-J \\ (\ell\neq\lambda)}}^{J} \frac{\epsilon_1(1-\epsilon_2)^2}{(\eta-a_\ell)^2} F(x, y-a_\ell - \frac{1}{\eta-a_\ell}, z) \right\} \Gamma(\eta) d\eta$$

$$+ \frac{2}{\pi} \sum_{m=1}^{\infty} \sin m\theta_\lambda \int_0^\infty I_m(kr_\lambda) \sin kx \, dk \left\{ \int_{b_{2\lambda+1}}^{b_{2\lambda}} + \int_{b_{2\lambda-1}}^{b_{2\lambda-\eta}} S_m^{(j)}(k, \eta-a_\lambda)\Gamma d\eta \right.$$

$$\left. + \int_{b_{2\lambda}}^{b_{2\lambda-1}} T_m^{(j)}(k, \eta-a_\lambda)\Gamma d\eta \right\} , \tag{54b}$$

where in the second term of (54a), the sign $\sum''$ denotes the sum over ℓ except when $\ell = \nu$ for $\eta > 0$ and $\ell = -\nu$ for $\eta < 0$ (i. e., the νth jet pair are deleted in the ℓ-summation. In the above equations $F(x, y, z)$ is given in (26d) and $S_m^{(o)}$, $S_m^{(j)}$, $T_m^{(o)}$, $T_m^{(j)}$ by (22) and (25). The variables r_ℓ, θ_ℓ are defined by

$$y - a_\ell = r_\ell \cos\theta_\ell, \quad z = r_\ell \cos\theta_\ell, \quad \ell = -J, \ldots -1, 1, \ldots, J. \tag{54c}$$

3. The Fourier Expansion for Circulation; Lift Distribution

The spanwise lift distribution $\ell(y)$ and the total lift L are again given by (28) and (29). The circulation distribution $\Gamma(y)$, and hence the local lift $\ell(y)$, is assumed here to be an even function of y, that is, $\Gamma(-y) = \Gamma(y)$. In order that the pressure and the local lift shall be continuous at the jet boundaries, $y = b_1, b_2, \ldots, b_{2J}$, the following conditions (similar to 30)

$$\Gamma(b_\nu - 0) = \begin{Bmatrix} \mu \\ 1/\mu \end{Bmatrix} \Gamma(b_\nu + 0) \quad \text{for} \begin{cases} \nu = 1, 3, \ldots 2J-1, \\ \nu = 2, 4, \ldots 2J, \end{cases} \tag{55}$$

must therefore be satisfied. The continuity of the downwash at the jet boundaries will be examined later in the analysis.

The circulation $\Gamma(y)$ of the present case is assumed to have the following Fourier expansion

$$\Gamma(y) = 4V_j \Gamma_\nu(y), \quad \text{for } b_{\nu+1} < |y| \leq b_\nu, \quad \nu = 0, 1, 2, \ldots, 2J, \tag{56a}$$

$$\Gamma_o(y) = \sum_{n=0}^{N_o - 1} A_{2n+1}^{(0)} \sin(2n+1)\psi_o, \tag{56b}$$

$$\Gamma_\nu(y) = \Gamma_{\nu-1}(y) + A_o^{(\nu)} + \sum_{n=0}^{N_\nu - 1} A_{2n+1}^{(\nu)} \sin (2n+1)\psi_\nu, \quad \nu = 1, 2, \ldots, 2J. \quad (56c)$$

The last two equations may also be combined to give

$$\Gamma_\nu(y) = \sum_{s=0}^{\nu} \left\{ A_o^{(s)} + \sum_{n=0}^{N_s - 1} A_{2n+1}^{(s)} \sin (2n+1)\psi_s \right\} \text{ for } \nu = 0, 1, 2, \ldots, 2J, \quad (56d)$$

$A_o^{(0)} = 0$ being understood. The above expansion gives $\Gamma(y)$ an even function of y, as clearly suggested by the fact that the downwash $w(y)$ will be symmetrical (even in the presence of slipstream rotation) about the plane $y = 0$.

It should be mentioned here that a few different expansions for $\Gamma(y)$ have been examined by the authors by performing several numerical programs on an IBM-709 machine. One of these expansions is particularly worth noting. This expansion assumes the same form as (56) except that in (56c) the term $\Gamma_{\nu-1}(y)$ is removed. This reduces the number of terms of the expansion in the inner regions R_ν, $\nu \geq 1$. Thus the series with coefficients $A_{2n+1}^{(\nu)}$ is assigned only to the region R_ν, in which $b_{\nu+1} < |y| \leq b_\nu$, or $0 \leq \psi_\nu < \beta_\nu^{(\nu+1)}$ and $\pi - \beta_\nu^{(\nu+1)} < \psi_\nu \leq \pi$. Strictly speaking, these series in this type of expansion are not Fourier series since the set of functions $\sin (2n+1)\psi_\nu$ are not mutually orthogonal over the region R_ν. It has been found that this type of expansion induces numerical instability in the computing program. The expansion (56), however, has been found satisfactory.

Now application of conditions (55) to (56) yields

$$A_o^{(\nu)} = \begin{Bmatrix} (\mu - 1) \\ (\frac{1}{\mu} - 1) \end{Bmatrix} \left\{ \sum_{s=0}^{\nu-1} \left[A_o^{(s)} + \sum_{n=0}^{N_s - 1} A_{2n+1}^{(s)} \sin (2n+1)\beta_s^{(\nu)} \right] \right\} \quad (57)$$

$$\text{for } \begin{cases} \nu = 1, 3, \ldots, 2J-1, \\ \nu = 2, 4, \ldots, 2J, \end{cases}$$

in which $A_o^{(0)} = 0$. Thus the total number of the arbitrary coefficients $A_{2n+1}^{(\nu)}$ is

$$\sum_{s=0}^{2J} N_s = N_o + N_1 + \ldots + N_{2J} . \tag{58}$$

The total lift L is obtained by integrating $\ell(y)$ along the span,

$$\frac{L}{8\rho V_j^2} = \frac{1}{4V_j^2} \int_0^{b_o} V_{local}\, \Gamma(y)dy = \mu \sum_{\nu=0,1\ldots}^{2J} \int_{b_{\nu+1}}^{b_\nu} \Gamma_\nu(y)\, dy$$

$$+ (1-\mu) \sum_{\nu=1}^{J} \int_{b_{2\nu}}^{b_{2\nu-1}} \Gamma_{2\nu-1}(y)\, dy$$

On substituting (56d) in the above integrals, and making use of $b_{2\nu-1} - b_{2\nu} = 2$ (which is the diameter of the jet), we obtain

$$\frac{L}{8\rho V_j^2} = \mu \sum_{\nu=0}^{2J} b_\nu [A_o^{(\nu)} + \frac{\pi}{4} A_1^{(\nu)}] + (1-\mu) \sum_{\nu=1}^{J} \sum_{s=0}^{2\nu-1} \Big\{ 2A_o^{(s)} + \frac{b_s}{2} A_1^{(s)} [\beta_s^{(2\nu)} - \beta_s^{(2\nu-1)}]$$

$$+ \frac{b_s}{2} \Big[\sum_{n=1}^{N_s - 1} (A_{2n+1}^{(s)} - A_{2n-1}^{(s)}) \frac{\sin 2n\beta_s^{(2\nu)} - \sin 2n\beta_s^{(2\nu-1)}}{2n}$$

$$- A_{2N_s-1}^{(s)} \frac{\sin 2N_s\beta_s^{(2\nu)} - \sin 2N_s \beta_s^{(2\nu-1)}}{2N_s} \Big] \Big\} . \tag{59}$$

4. Downwash Distribution

Again we let $c(y)$ be the half-chord length of the wing at station y. Then the downwash at the three-quarter chord can be derived from the solution (54) by differentiation,

$$w_o(y) = -\frac{\partial}{\partial z}\varphi_o(c, y, 0) \quad \text{for} \quad b_{2\lambda+1} < |y| \leqslant b_{2\lambda}, \quad \lambda = 0, 1, \ldots, J;$$
$$\tag{60}$$
$$w_{j,\lambda}(y) = -\frac{\partial}{\partial z}\varphi_{j,\lambda}(c, y, 0) \quad \text{for} \quad b_{2\lambda} < |y| \leqslant b_{2\lambda-1}, \quad \lambda = 1, 2, \ldots, J.$$

On integration by parts of those integrals in the expression for $\partial\varphi(c, y, 0)/\partial z$ which contain F_z, and by making use of (36), (37) and (7), we find that those terms containing $G(y-\eta)$, when evaluated at various limits of integration, all vanish by virtue of (55) and (7a), and we finally obtain

$$4\pi w_o(y) = \sum_{\nu=0}^{2J}(1-\delta_\nu^{odd}\epsilon_2)\int_{b_{\nu+1}}^{b_\nu}[G(y-\eta, c) - G(y+\eta, c)]\frac{d\Gamma}{d\eta}d\eta$$

$$-\epsilon_1\sum_{\nu=0}^{J}\sum_{\ell=-J}^{J}\int_{b_{2\nu+1}}^{b_{2\nu}}[G(y-a_\ell-\frac{1}{\eta-a_\ell}, c) - G(y+a_\ell+\frac{1}{\eta-a_\ell}, c)]\frac{d\Gamma}{d\eta}d\eta$$

$$-\epsilon_1(1-\epsilon_2)\sum_{\nu=1}^{J}\sum_{\substack{\ell=-J \\ (\ell\neq\nu)}}^{J}{}'\int_{b_{2\nu}}^{b_{2\nu-1}}[G(y-a_\ell-\frac{1}{\eta-a_\ell}, c) - G(y+a_\ell+\frac{1}{\eta-a_\ell}, c)]\frac{d\Gamma}{d\eta}d\eta$$

$$+ 4\pi w_o^*, \tag{61a}$$

$$4\pi w_o^*(y) = \frac{\epsilon_1^2}{\mu} \sum_{\nu=1}^{J} \sum_{\substack{\ell=-J \\ (\ell\neq\nu)}}^{J}{}' \Gamma(b_{2\nu}+0)\left[G(y-a_\ell - \frac{1}{b_{2\nu}-a_\ell}, c) - G(y+a_\ell + \frac{1}{b_{2\nu}-a_\ell}, c)\right]$$

$$-\epsilon_1^2 \sum_{\nu=1}^{J} \sum_{\substack{\ell=-J \\ (\ell\neq\nu)}}^{J} \Gamma(b_{2\nu-1}+0)\left[G(y-a_\ell - \frac{1}{b_{2\nu-1}-a_\ell}, c) - G(y+a_\ell + \frac{1}{b_{2\nu-1}-a_\ell}, c)\right]$$

$$-\frac{2}{\pi} \sum_{\ell=-J}^{J} \sum_{m=1}^{\infty} m \int_0^\infty \frac{K_m(k(y-a_\ell))}{y-a_\ell} \sin kc \, dk \left\{ \int_{b_{2\ell+1}}^{b_{2\ell}} \right.$$

$$\left. + \int_{b_{2\ell-1}}^{b_{2\ell-2}} S_m^{(o)}(k, \eta-a_\ell)\Gamma \, d\eta + \int_{b_{2\ell}}^{b_{2\ell-1}} T_m^{(o)}(k, \eta-a_\ell)\Gamma \, d\eta \right\} ;$$

$$4\pi w_{j,\lambda}(y) = (1-\epsilon_2) \sum_{\nu=0}^{2J} (1-\delta_\nu^{odd}\epsilon_2) \int_{b_{\nu+1}}^{b_\nu} [G(y-\eta, c) - G(y+\eta, c)] \frac{d\Gamma}{d\eta} d\eta$$

$$+ \epsilon_1 \int_{b_{2\lambda}}^{b_{2\lambda-1}} \left[\epsilon_1 G(y-\eta, c) + (2-\epsilon_1^2) G(y-a_\lambda - \frac{1}{\eta-a_\lambda}, c) \right.$$

$$\left. - (1-\epsilon_1^2) \sum_{\ell=-J}^{J} G(y-a_\ell - \frac{1}{\eta-a_\ell}, c) \right] \frac{d\Gamma}{d\eta} d\eta$$

$$- \epsilon_1(1-\epsilon_2) \sum_{\nu=0}^{J} \sum_{\substack{\ell=-J \\ (\ell\neq\lambda)}}^{J}{}' \int_{b_{2\nu+1}}^{b_{2\nu}} \left[G(y-a_\ell - \frac{1}{\eta-a_\ell}, c) - G(y-a_\ell + \frac{1}{\eta+a_\ell}, c)\right] \frac{d\Gamma}{d\eta} d\eta$$

$$+ 4\pi w_{j,\lambda}^* , \qquad (61b)$$

$$4\pi w^*_{j,\lambda}(y) = -\epsilon_1(1-\epsilon_1^2)\sum_{\substack{\ell=-J \\ (\ell\neq\lambda)}}^{J}{}' \Big[\Gamma(b_{2\lambda}+0)G(y-a_\ell - \frac{1}{b_{2\lambda}-a_\ell}, c)$$

$$-\mu\Gamma(b_{2\lambda-1}+0)G(y-a_\ell - \frac{1}{b_{2\lambda-1}-a_\ell}, c)\Big]$$

$$+\epsilon_1(1+\epsilon_1)\sum_{\nu=1}^{J}\sum_{\substack{\ell=-J \\ (\ell\neq\lambda,\nu)}}^{J}{}' \Gamma(b_{2\nu}+0)\Big[G(y-a_\ell - \frac{1}{b_{2\nu}-a_\ell}, c) - G(y-a_\ell + \frac{1}{b_{2\nu}+a_\ell}, c)\Big]$$

$$-\epsilon_1(1-\epsilon_2)\sum_{\nu=1}^{J}\sum_{\substack{\ell=-J \\ (\ell\neq\lambda,\,\nu)}}^{J}{}' \Gamma(b_{2\nu-1}+0)\Big[G(y-a_\ell - \frac{1}{b_{2\nu-1}-a_\ell}, c) - G(y-a_\ell + \frac{1}{b_{2\nu-1}+a_\ell}, c)\Big]$$

$$-\frac{2}{\pi}\sum_{m=1}^{\infty} m \int_0^{\infty} \frac{I_m(k(y-a_\lambda))}{y-a_\lambda} \sin kc\, dk \Big\{ \int_{b_{2\lambda+1}}^{b_{2\lambda}}$$

$$+\int_{b_{2\lambda-1}}^{b_{2\lambda-2}} S_m^{(j)}(k, \eta-a_\lambda)\Gamma\, d\eta + \int_{b_{2\lambda}}^{b_{2\lambda-1}} T_m^{(j)}(k, \eta-a_\lambda)\Gamma\, d\eta \Big\} .$$

In (61a) and (61b), the notation δ_ν^{odd} is defined by $\delta_\nu^{odd} = 1$ if ν is an odd integer and $= 0$ if ν is an even integer. In the expressions for w_o^* and $w^*_{j,\lambda}$, the terms with $G(y \pm a_\ell \pm (b_\nu - a_\ell)^{-1}, c)$ arise from the fact that the reflections of the image systems are not complete; these terms will be removed if all higher order images are included in the solution of φ. However, it is noted that these G functions are regular in their respective regions, and their magnitudes, with their multiplication factors (depending on μ, ϵ_1 or ϵ_2) accounted for, are generally very small. Furthermore, it has been found from the numerical results that the contributions of the

Fourier-Bessel series in w_o^* and $w_{j,\lambda}^*$ are also small. Hence w_o^* and $w_{j,\lambda}^*$ are rather unimportant compared with the remaining terms in the expression for w_o and $w_{j,\lambda}$.

Now from (51) and (56d) we find

$$\frac{d\Gamma}{d\eta}\,d\eta = \frac{d\Gamma}{d\psi_s}\,d\psi_s = 4V_j \sum_{s=0}^{\nu} \sum_{n=0}^{N_s-1} (2n+1)A_{2n+1}^{(s)} \cos(2n+1)\psi_s d\psi_s \qquad (62)$$

for $b_{\nu+1} < |y| \leq b_\nu$,

$\nu = 0, 1, \ldots, 2J.$

Using this expression for $\Gamma' d\eta$ and (36) for G, we find that some of the resulting integrals which contain $G_1(y-\eta)$ and $G_1(y+\eta)$ can be evaluated in closed form. The final result is given in the following. Since $w(y)$ is evidently an even function of y, only the result for positive y will be given here.

a. Outside the Jets, $b_{2\lambda+1} < y \leq b_{2\lambda}$, $\lambda = 0, 1, \ldots, J$

$$\frac{w_o(y)}{V_j} = 2\sum_{s=0}^{2\lambda} \sum_{n=1,3,\ldots}^{2N_s-1} \frac{nA_n^{(s)}}{b_s} \frac{\sin n\psi_s}{\sin\psi_s}$$

$$- 2(1-\delta_\lambda^J) \sum_{s=2\lambda+1}^{2J} (1-\delta_s^{(2\lambda+1)}\epsilon_2) \sum_{n=1,3,\ldots}^{2N_s-1} \frac{nA_n^{(s)}}{b_s} \frac{[y/b_s - \sqrt{(y/b_s)^2-1}]^n}{\sqrt{(y/b_s)^2-1}}$$

$$- \epsilon_2 \sum_{\nu=1}^{J} \sum_{s=0}^{2\nu-1} \sum_{n=1,3,\ldots}^{2N_s-1} \frac{nA_n^{(s)}}{b_s} (1-\delta_\nu^{(\lambda+1)}\delta_s^{(2\lambda+1)})[P_n^{(s)}(\frac{y}{b_s};R_{2\nu-1})$$

$$+ P_n^{(s)}(-\frac{y}{b_s};R_{2\nu-1})]$$

$$+\epsilon_2(1-\delta_\lambda^J)\sum_{n=1,3,\ldots}^{(2N_{2\lambda+1}-1)} \frac{nA_n^{(s)}}{b_{2\lambda+1}}\Big[P_n^{(2\lambda+1)}\Big(\frac{y}{b_{2\lambda+1}};\sum_{\nu=2\lambda+2}^{2J} R_\nu\Big)$$

$$+P_n^{(2\lambda+1)}\Big(-\frac{y}{b_{2\lambda+1}};\sum_{\nu=2\lambda+2}^{2J} R_\nu\Big)\Big]$$

$$+\sum_{\nu=0}^{2J}(1-\delta_\nu^{odd}\epsilon_2)\sum_{s=0}^{\nu}\sum_{n=1,3,\ldots}^{2N_s-1}\frac{nA_n^{(s)}}{b_s}\Big[\Omega_n^{(s)}\Big(\frac{y}{b_s};\frac{b_s}{c};R_\nu\Big)$$

$$+\Omega_n^{(s)}\Big(\frac{-y}{b_s};\frac{b_s}{c};R_\nu\Big)\Big]$$

$$-\epsilon_1\sum_{\nu=0}^{2J}(1-\delta_\nu^{odd}\epsilon_2)\sum_{\ell=-J}^{J}(1-\delta_\nu^{odd}\delta_\ell^{(\nu+1)/2})\sum_{s=0}^{\nu}\sum_{n=1,3,\ldots}^{2N_s-1} nA_n^{(s)}\Big[Q_n^{(s)}(y;a_\ell;R_\nu)$$

$$+Q_n^{(s)}(-y;a_\ell;R_\nu)+\Lambda_n^{(s)}(y;a_\ell;R_\nu)+\Lambda_n^{(s)}(-y;a_\ell;R_\nu)\Big]+\frac{w_o^*(y)}{V_j}\,. \qquad (63a)$$

b. <u>Inside the λth Jet, $b_{2\lambda}<y\le b_{2\lambda-1}$, $\lambda=1,2,\ldots,J$</u>

$$\frac{w_{j,\lambda}(y)}{V_j}=2\sum_{s=0}^{2\lambda-1}\sum_{n=1,3,\ldots}^{2N_s-1}\frac{nA_n^{(s)}}{b_s}\,\frac{\sin n\psi_s}{\sin\psi_s}$$

$$-2(1-\epsilon_2)\sum_{s=2\lambda}^{2J}(1-\epsilon_2+\delta_s^{2\lambda}\epsilon_2)\sum_{n=1,3,\ldots}^{2N_s-1}\frac{nA_n^{(s)}}{b_s}\,\frac{\left[y/b_s-\sqrt{(y/b_s)^2-1}\,\right]^n}{\sqrt{(y/b_s)^2-1}}$$

$$-\epsilon_1^2\sum_{s=0}^{2\lambda-1}\sum_{n=1,3,\ldots}^{2N_s-1}\frac{nA_n^{(s)}}{b_s}\Big[P_n^{(s)}\Big(\frac{y}{b_s};\sum_{\nu=0}^{2\lambda-2}R_\nu\Big)+P_n^{(s)}\Big(\frac{y}{b_s};\sum_{\nu=2\lambda}^{2J}R_\nu\Big)$$

$$+P_n^{(s)}\Big(-\frac{y}{b_s};\sum_{\nu=0}^{2J}R_\nu\Big)\Big]-\epsilon_2(1-\epsilon_2)(1-\delta_\lambda^J)\sum_{n=1,3,\ldots}^{(2N_{2\lambda+1}-1)}\frac{nA_n^{(s)}}{b_{2\lambda}}\Big[P_n^{(2\lambda)}\Big(\frac{y}{b_{2\lambda}};\sum_{\nu=2\lambda+1}^{2J}R_\nu\Big)$$

$$+ P_n^{(2\lambda)}\left(-\frac{y}{b_s};\sum_{\nu=2\lambda+1}^{2J} R_\nu\right)\Big] + \epsilon_2(1-\epsilon_2)\sum_{\nu=0}^{J}\sum_{s=0}^{2\nu}\sum_{n=1,3,\ldots}^{2N_s-1}\frac{nA_n^{(s)}}{b_s}(1-\delta_\nu^\lambda\delta_s^{2\lambda})$$

$$\times\left[P_n^{(s)}\left(\frac{y}{b_s};R_{2\nu}\right)+P_n^{(s)}\left(-\frac{y}{b_s};R_{2\nu}\right)\right]$$

$$-(1-\epsilon_2)\sum_{\nu=0}^{2J}(1-\delta_\nu^{odd}\epsilon_2)\sum_{s=0}^{\nu}\sum_{n=1,3,\ldots}^{2N_s-1}\frac{nA_n^{(s)}}{b_s}\left[\Omega_n^{(s)}\left(\frac{y}{b_s};\frac{b_s}{c};R_\nu\right)\right.$$

$$\left.+\Omega_n^{(s)}\left(-\frac{y}{b_s};\frac{b_s}{c};R_\nu\right)\right]+\epsilon_1^2\sum_{s=0}^{2\lambda-1}\sum_{n=1,3}^{2N_s-1}\frac{nA_n^{(s)}}{b_s}\Omega_n^{(s)}\left(\frac{y}{b_s};\frac{b_s}{c};R_{2\lambda-1}\right)$$

$$-\epsilon_1\sum_{s=0}^{2\lambda-1}\sum_{n=1,3}^{2N_s-1}nA_n^{(s)}\sum_{\ell=-J}^{J}\Big\{[1-\epsilon_1^2-\delta_\ell^\lambda(2-\epsilon_1^2)][Q_n^{(s)}(y;a_\ell;R_{2\lambda-1})$$

$$+\Lambda_n^{(s)}(y;a_\ell;R_{2\lambda-1})]\Big\}-\epsilon_1(1-\epsilon_2)\sum_{\nu=0}^{J}\sum_{s=0}^{2\nu}\sum_{n=1,3}^{2N_s-1}nA_n^{(s)}\sum_{\ell=-J}^{J}(1-\delta_\ell^\lambda)$$

$$\times[Q_n^{(s)}(y;a_\ell;R_{2\nu})+Q_n^{(s)}(-y;-a_\ell;R_{2\nu})+\Lambda_n^{(s)}(y;a_\ell;R_{2\nu})+\Lambda_n^{(s)}(-y;-a_\ell;R_{2\nu})]$$

$$+\frac{w_{j,\lambda}^*(y)}{V_j}\quad. \tag{63b}$$

In the above equations, w_o^* and $w_{j,\lambda}^*$ are given in (61); δ_n^m are the Kronecker deltas,

$$\delta_n^m = 1 \text{ if } m = n \text{ and } \delta_n^m = 0 \text{ if } m \neq n\,; \tag{63c}$$

and the functions P, Q, Ω, Λ are defined as

$$P_n^{(s)}(y/b_s;R_\nu) = \frac{2}{\pi}\int_{\beta_s^{(\nu)}}^{\beta_s^{(\nu+1)}}\frac{\cos n\theta\, d\theta}{\cos\theta - y/b_s}\,, \tag{64a}$$

$$Q_n^{(s)}(y;a_\ell;R_\nu) = \frac{2}{\pi}\int_{\beta_s^{(\nu)}}^{\beta_s^{(\nu+1)}}\frac{(b_s\cos\theta - a_\ell)\cos n\theta\, d\theta}{1+(b_s\cos\theta - a_\ell)(a_\ell - y)}\,, \tag{64b}$$

$$\Omega_n^{(s)}\left(\frac{y}{b_s};\frac{b_s}{c};R_\nu\right) = \frac{1}{\pi}\left(\frac{b_s}{c}\right)^2 \int_{\beta_s^{(\nu)}}^{\beta_s^{(\nu+1)}} \frac{(\cos\theta - y/b_s)\cos n\theta\, d\theta}{1+\left[1+\left(\frac{b_s}{c}\right)^2\left(\cos\theta - \frac{y}{b_s}\right)^2\right]^{1/2}}, \qquad (64c)$$

$$\Lambda_n^{(s)}(y;a_\ell;R_\nu) = \frac{1}{\pi c^2}\int_{\beta_s^{(\nu)}}^{\beta_s^{(\nu+1)}} \frac{\left(\frac{1}{b_s\cos\theta - a_\ell} + a_\ell - y\right)\cos n\theta\, d\theta}{1+\left[1+\frac{1}{c^2}\left(\frac{1}{b_s\cos\theta - a_\ell} + a - y\right)^2\right]^{1/2}}. \qquad (64d)$$

The strongest singularities which appear in the expression (63) for $w(y)$ are the square root singularities at $y = b_s$, $s = 1, 2, \ldots, 2J$. In order that these singularities at the jet boundaries be removed, the following $2J$ relations

$$\sum_{n=1,3,\ldots}^{2N_s-1} nA_n^{(s)} = 0, \quad s = 1, 2, \ldots, 2J \qquad (65)$$

must be satisfied.

Further, it is noted that the functions $P_n^{(s)}$ and $Q_n^{(s)}$ may have logarithmic singularities at the jet boundary. These singularities are listed below.

1. In $b_{2\lambda+1} < y \leq b_{2\lambda}$, $\lambda = 0, 1, \ldots, J$,

$$P_n^{(s)}\left(\frac{b_{2\lambda+1}+\epsilon}{b_s}; R_{2\lambda+1}\right) \cong b_s Q_n^{(s)}(b_{2\lambda+1}+\epsilon; a_{\lambda+1}; R_{2\lambda})$$

$$\cong \frac{2}{\pi}\frac{\cos n\beta_s^{2\lambda+1}}{\sin\beta_s^{2\lambda+1}}\log\epsilon, \qquad (66a)$$

$$P_n^{(s)}\left(\frac{b_{2\lambda}-\epsilon}{b_s}; R_{2\lambda-1}\right) \cong b_s Q_n^{(s)}(b_{2\lambda}-\epsilon; a_\lambda; R_{2\lambda})$$

$$\cong -\frac{2}{\pi}\frac{\cos n\beta_s^{2\lambda}}{\sin\beta_s^{2\lambda}}\log\epsilon\ ; \qquad (66b)$$

2. In $b_{2\lambda} < y \leq b_{2\lambda-1}$, $\lambda = 1, 2, \ldots, J$,

$$P_n^{(s)}\left(\frac{b_{2\lambda}+\epsilon}{b_s}; R_{2\lambda}\right) \cong b_s Q_n^{(s)}(b_{2\lambda}+\epsilon; a_\lambda; R_{2\lambda-1})$$

$$\cong \frac{2}{\pi} \frac{\cos n\beta_s^{2\lambda}}{\sin \beta_s^{2\lambda}} \log \epsilon \,, \tag{66c}$$

$$P_n^{(s)}\left(\frac{b_{2\lambda-1}-\epsilon}{b_s}; R_{2\lambda-2}\right) \cong b_s Q_n^{(s)}(b_{2\lambda-1}-\epsilon; a_\lambda; R_{2\lambda-1})$$

$$\cong -\frac{2}{\pi} \frac{\cos n\beta_s^{2\lambda-1}}{\sin \beta_s^{2\lambda-1}} \log \epsilon \,. \tag{66d}$$

To remove these singularities we impose the following conditions

$$\sum_{s=0}^{2\lambda-2} \sum_{n=1,3,\ldots}^{2N_s-1} \frac{nA_n^{(s)}}{b_s} \cos n\beta_s^{2\lambda-1}/\sin \beta_s^{2\lambda-1} = 0, \quad \lambda = 1, 2, \ldots J \,; \tag{67a}$$

$$\sum_{s=0}^{2\lambda-1} \sum_{n=1,3,\ldots}^{2N_s-1} \frac{nA_n^{(s)}}{b_s} \cos n\beta_s^{2\lambda}/\sin \beta_s^{2\lambda} = 0, \quad \lambda = 1, 2, \ldots J. \tag{67b}$$

By making use of the conditions (65) and (67) we may introduce in (63) the following substitutions:

$$\left[\frac{y}{b_s} - \sqrt{\left(\frac{y}{b_s}\right)^2 - 1}\,\right]^n \Big/ \sqrt{\left(\frac{y}{b_s}\right)^2 - 1} \quad \text{by} \quad \left\{\left[\frac{y}{b_s} - \sqrt{\left(\frac{y}{b_s}\right)^2 - 1}\,\right]^n - 1\right\} \Big/ \sqrt{\left(\frac{y}{b_s}\right)^2 - 1} \,,$$

in $b_{2\lambda+1} < y \leq b_{2\lambda}$, $\lambda = 0, 1, \ldots J$,

$$P_n^{(s)}\left(\frac{y}{b_s}; R_{2\lambda+1}\right) \text{ by } P_n^{*(s)}\left(\frac{y}{b_s}; R_{2\lambda+1}\right)$$

$$= \frac{2}{\pi} \int_{\beta_s^{2\lambda+1}}^{\beta_s^{2\lambda+2}} \frac{\cos n\theta - \cos n\beta_s^{2\lambda+1}}{\cos\theta - y/b_s} \, d\theta \,,$$

$P_n^{(s)}(\frac{y}{b_s}; R_{2\lambda-1})$ by $P_n^{*(s)}(\frac{y}{b_s}; R_{2\lambda-1})$

$$= \frac{2}{\pi}\int_{\beta_s^{2\lambda-1}}^{\beta_s^{2\lambda}} \frac{\cos n\theta - \cos n\beta_s^{2\lambda}}{\cos\theta - y/b_s}\, d\theta ,$$

$Q_n^{(s)}(y;a_{\lambda+1};R_{2\lambda})$ by $Q_n^{*(s)}(y;a_{\lambda+1};R_{2\lambda})$

$$= \frac{2}{\pi}\int_{\beta_s^{2\lambda}}^{\beta_s^{2\lambda+1}} \frac{(b_s\cos\theta - a_{\lambda+1})(\cos n\theta - \cos n\beta_s^{2\lambda+1})}{1 + (b_s\cos\theta - a_{\lambda+1})(a_{\lambda+1} - y)}\, d\theta ,$$

$Q_n^{(s)}(y;a_\lambda;R_{2\lambda})$ by $Q_n^{*(s)}(y;a_\lambda;R_{2\lambda})$

$$= \frac{2}{\pi}\int_{\beta_s^{2\lambda}}^{\beta_s^{2\lambda+1}} \frac{(b_s\cos\theta - a_\lambda)(\cos n\theta - \cos n\beta_s^{2\lambda})}{1 + (b_s\cos\theta - a_\lambda)(a_\lambda - y)}\, d\theta$$

together with similar substitutions in $b_{2\lambda} < y \leq b_{2\lambda-1}$, $\lambda = 1, 2, \ldots, J$. After these substitutions are made, the downwash $w(y)$ then becomes bounded everywhere over the wing. There are $2J$ conditions of the form (67) in total.

5. Application of Boundary Condition on the Wing

The same assumptions for the effect of slipstream rotation as stated previously in Section B4 will be retained for the present case of multiple jets. Since $w(y)$ is even in y, the boundary condition need be applied for positive y only. Hence if $\alpha(y)$ is the local geometrical angle of attack at y of the $3/4$ chord line, then, by the Weissinger method, the required boundary condition becomes

$$w_o(y)/V_j = \mu\alpha(y) \quad \text{for} \quad b_{2\lambda+1} < y \leq b_{2\lambda}, \quad \lambda = 0, 1, \ldots, J, \tag{68a}$$

$$w_{j,\lambda}(y)/V_j = \alpha(y) + \frac{(y-a_\lambda)\omega(y-a_\lambda)}{V_j} \quad \text{for} \quad b_{2\lambda} < y \leq b_{2\lambda-1},$$

$$\lambda = 1, 3, \ldots, J. \tag{68b}$$

where ω is an even function of its argument and represents the slipstream rotation, the convention for the sign of ω being already specified in Section B4.

Here we have $\sum_{s=0}^{2J} N_s$ unknown coefficients $A_{2n+1}^{(s)}$ which must also obey the $2J$ constraints (65) and 2J constraints (67). Therefore we may choose appropriately $(\Sigma N_s - 4J)$ points on the $3/4$ chord line at which we apply condition (68).

III. COMPUTATIONAL RESULTS

The problem of verifying the theory is two-fold. First, an involved procedure for electronic machine computations must be developed to produce numerical results to apply the theory. Second, experimental data providing spanwise lift distributions for applicable wing configurations is required.

Major strides were taken in the computational programming of the theoretical multiple jet relations developed in this paper. This program was designed for the IBM Type 709 electronic computer, and applied at the UCLA facility. It should be recognized that the mathematical formulation and the computing procedure are highly interrelated. In developing the mathematical theory, the approach and selection of system coordinates must be compatible with the available computing techniques. However, all of the computational difficulties cannot initially be foreseen and this results in various modifications in the mathematical form of presentation during the development of a satisfactory computational procedure.

The mathematical formulation presented in this paper yielded slight numerical inconsistencies on several occasions. It is felt, however, that the trends exhibited by the computed results are reasonable. An improved formulation which shows promise of relieving some of the numerical difficulties is presently under investigation. Much of the computational program utilized in this paper would be applicable to the new formulation.

Suitable experimental data for verification of the theory is sadly lacking. In September of 1959, NASA (Ames Research Center, Moffett

Field, Calif.) published an account of force measurements of a multi-jet configuration[16]. Limited spanwise measurements were made during the test, the data for which was not published in their report. These Ames spanwise measurements were obtained upon request but were not suitable for correlation with the theory. Nevertheless, the basic geometry of their model was employed in an example computation based on the present theory.

The Ames test was not primarily concerned with spanwise loading and thus only a limited number of spanwise measurements were taken. The propeller slipstream velocity over the wing was also not measured. The effect of the fuselage, engine nacelles, and asymmetric loading between the right and left wing panels (spanwise measurements were made on the left wing panel only) also invalidate any spanwise comparison with the theory. Also integration of the Ames spanwise lift data did not agree with their total lift measurements for reasons enumerated above.

Fig. 4 presents theoretical curves for the spanwise lift distribution of the selected wing-jet arrangement (similar to Ames configuration). The aspect ratio is 10 and the taper ratio is 0.5. The angle of attack is 6° at the root chord and 0° at the tip. The spanwise location of the jets (propellers) is shown on the sketch at the top of the figure. The contribution of the Bessel function terms for this computation was found to be small and was accordingly disregarded.

The most significant trend observed in the theoretical curves is the increase in the local lift coefficient near the wing mid-span. This result is of primary importance for structural wing design.

The curves also show that lift is carried across the narrow strip between closely spaced jets. Also, when the jets are close together, their effects combine to produce a single peak. Obviously, if the jets are a sizeable distance apart, two distinct peaks will appear.

The maximum local lift coefficient occurs near the jet closest to the mid-span. This is reasonable since the local lift of the wing without jets increases toward the center. The washout twist distribution also amplifies this effect. The curves also show a significantly higher local lift in the region of the outer jet, particularly for the higher jet strengths (lower μ values).

Significantly, there is only one peak in each of the curves and this peak shifts towards the wing mid-span for high μ values. This is explained in terms of the relative strength of the wing and jet, i.e., the wing alone has its maximum local lift (peak) at the mid-span while the jet creates a peak at the jet center. Thus, the jet tends to pull the peak toward its center while the wing tends to pull the peak toward the wing centerline, resulting in a peak in between. Logically, this peak shifts toward the wing centerline for weak jets (high μ values).

IV. CONCLUSIONS

Lifting surface theory has been generalized to establish a foundation from which many problems concerned with the non-uniform aerodynamics of wing-jet interaction may be solved. This generalization has been applied to the case of a wing extending through multiple jets.

The multiple jet formulation was programmed on the IBM 709 electronic computer. Due to some slight numerical inconsistencies an improved formulation is presently under investigation. However, the trends indicated by the present formulation are considered to be valid.

The spanwise lift distribution of a wing extending through four (4) jets was computed (Fig. 4). A large increase in lift inboard and within the jets (propellers) was obtained with strong jets (low μ values). Significant increases in lift outboard of the jets are also apparent.

These results provide a basis for optimizing multi-jet wing-propeller configurations, for example by determining the lift distribution of a series of wings extending through a systematic family of multiple jet arrangements. As demonstrated in Ref. 2 the optimum planform for a wing extending through a single jet is finite and a similar result is anticipated for multiple jets.

The large lift magnification noted above resulting from the wing-propeller interaction has wide applicability in the area of V/STOL aircraft, particularly in the potential of large improvements in STOL capabilities.

V. RECOMMENDATIONS

Analytical solutions to the remaining two phases of the four phase fundamental program outlined in the Foreword are under way at the present time. With the generalization of the lifting surface theory presented in this report, the analytical solution of many secondary problems associated with the aerodynamics of wing-propeller interaction can readily be solved.

It is recommended that the analytical program be expanded to encompass further secondary factors so that Rethorst's basic solution and the generalization of this lifting surface theory presented in this report are fully exploited.

The most pressing immediate concern is the need for suitable multi-jet experimental data for correlation with the theory, and the need for a computational program of sufficient scope to delineate optimum configurations and gain an insight into all the ramifications of the analyses.

It is recommended that an intensive experimental investigation of spanwise lift distributions for wings extending through multiple jets be conducted. The experimental program should encompass all the configurations such as the highly cambered wing, tilt wing, etc., considered in the complete analytical program as outlined in the Foreword.

It is also recommended that the electronic computing program be greatly expanded to fully utilize the analytical results. It is emphasized that the computational program must proceed concurrently with the analytical development since the mathematical formulation must be compatible with computational programming techniques.

REFERENCES

1. Rethorst, S., "Aerodynamics of Nonuniform Flows as Related to an Airfoil Extending Through a Circular Jet," J. Aero. Sci. Vol. 25, No. 1, pp. 11-28, 1958.

2. Rethorst, S., Royce, W., and Wu, T. Y., "Lift Characteristics of Wings Extending Through Propeller Slipstreams," Vehicle Research Corporation Report No. 1, 1958.

3. Cumberbatch, Ellis, and Wu, T. Yao-tsu, "A Lifting Surface Theory for Wings Extending through Multiple Jets at High Angles of Attack," Vehicle Research Corporation Report No. 9, to be published.

4. Wu, T. Yao-tsu, "A Lifting Surface Theory for Wings Extending through Multiple Jets in Separated Flow Conditions," Vehicle Research Corporation Report No. 10, to be published.

5. Koning, C., "Influences of the Propeller on other Parts of the Airplane Structure," Aerodynamic Theory (Durand, F. W. Editor) Vol. 4, Div. M. Julius Springer, Berlin, 1935.

6. Graham, E. W., Lagerstrom, P. A., Licher, R. M., and Beane, B. J., "A Preliminary Theoretical Investigation of the Effects of Propeller Slipstream on Wing Lift," Douglas Aircraft Co. Report SM-14991, 1953.

7. Squire, H. B., and Chester, W., "Calculation of the Effect of Slipstream on Lift and Induced Drag," British ARC R and M no. 2368, 1950.

8. Weissinger, J., "Uber die Auftriebsverteilung von Pfeilflugeln," Forschungsbericht Nr. 1553, 1942. Also NACA TM 1120, 1947.

9. Smelt, R., and Davies, H., "Estimation of Increase in Lift Due to Slipstream," British ARC R and M No. 1788, 1937.

10. Stuper, J., "Einfluss des Schraubenstrahls auf Flugel und Leifwerk," Luftfahrtforschung, Vol. 15, No. 4, 1938. Also NACA TM 874, 1938.

11. Brenckmann, M. E., "Experimental Investigation of the Aerodynamics of a Wing in a Slipstream," J. Aero Sci., Vol. 25, No. 1, 1958.

12. Gobetz, F. W., "A Review of the Wing-Slipstream Problem with Experiments on a Wing Spanning a Circular Jet," Princeton University, Department of Aeronautical Engineering, Report 489, 1960.

13. Snedeker, Richard S., "Experimental Determination of Spanwise Lift Effects on a Wing of Infinite Aspect Ratio Spanning a Circular Jet," Princeton University, Department of Aeronautical Engineering, Report 525, 1961.

14. Kármán, Th. von. " Neue Darstellung der Tragflugeltheorie," Zeitschrift fur angewandte Mathmatik und Mechanik, Nr. 1/2, pp. 56-61, 1935. Also, Collected Works, Vol. 3, pp. 171-178, Butterworths Scientific Publications, 1956.

15. Watson, G. N., "Bessel Functions," Cambridge University Press, London, 1948.

16. Weiberg, James A., and Page, Robert V., "Large-Scale Wind-Tunnel Tests of an Airplane Model with an Unswept, Aspect-Ratio -10 Wing, Four Propellers, and Blowing Flaps," NASA TN D-25, September, 1959.

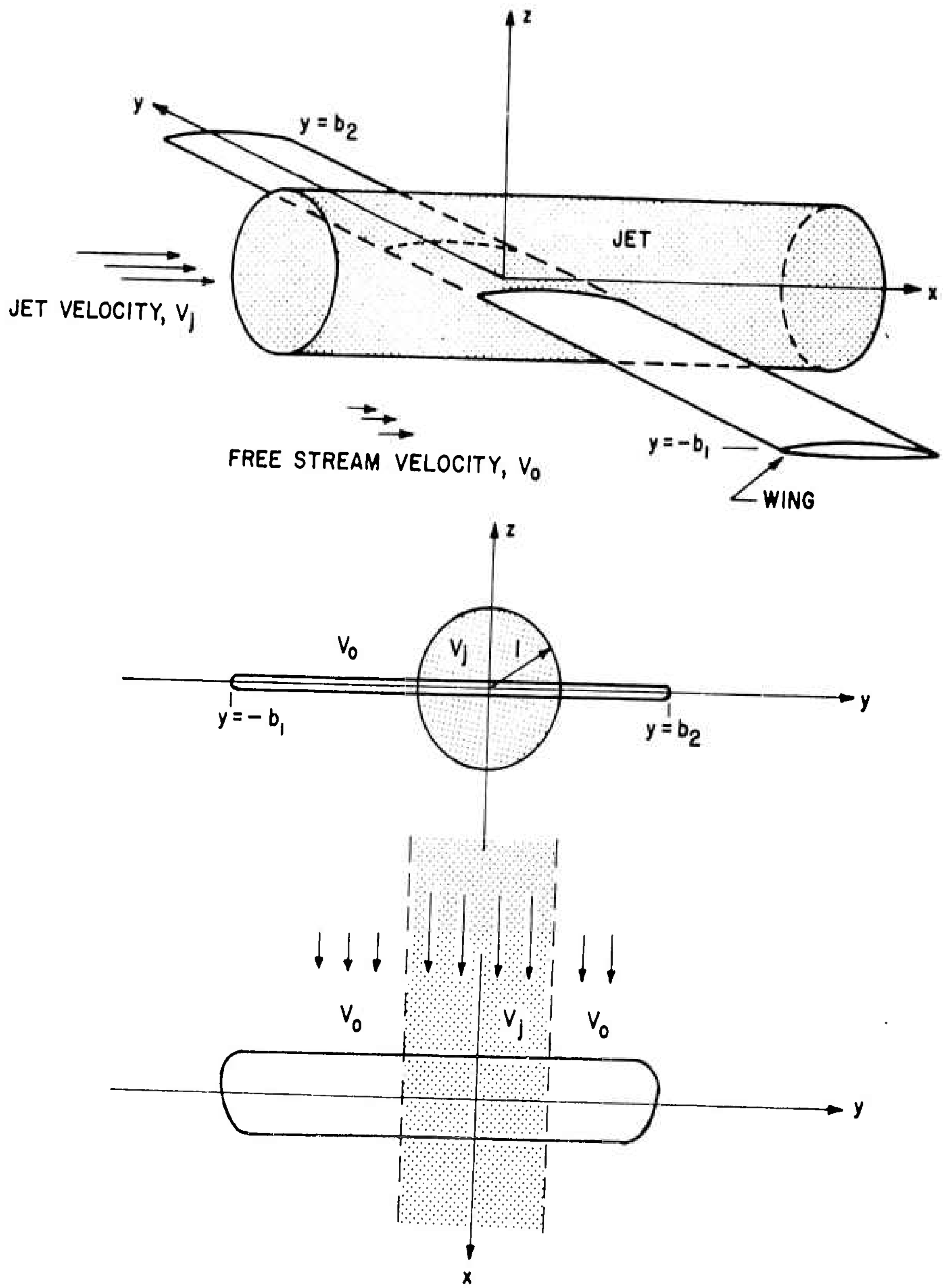
z
y
y = b_2
JET
x
JET VELOCITY, V_j
FREE STREAM VELOCITY, V_0
y = $-b_1$
WING
z
V_0
V_j
1
y
y = $-b_1$
y = b_2
V_0
V_j
V_0
y
x

FIG. 1

DEFINITION OF ANGULAR COORDINATES ψ_0 AND ψ_1

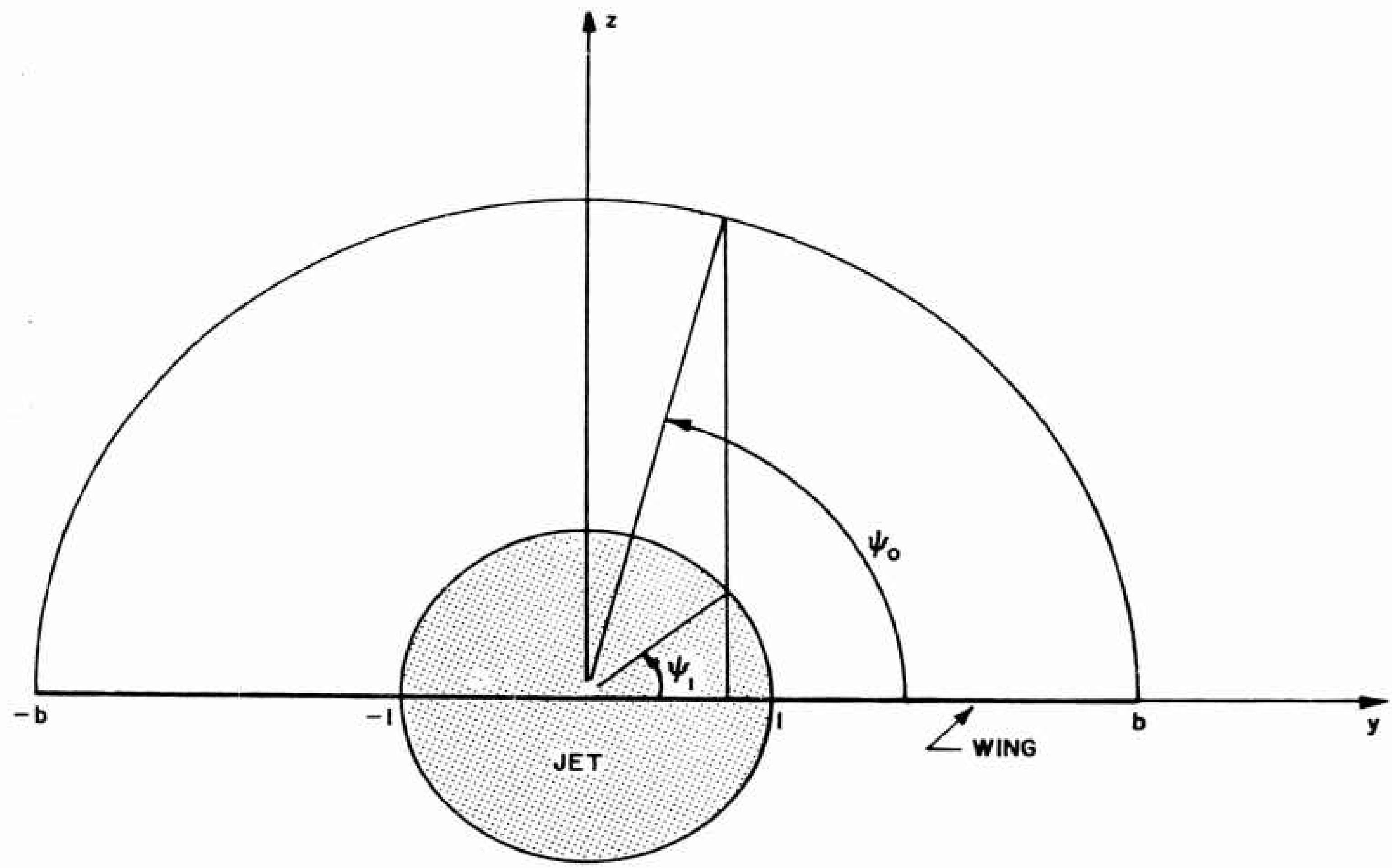

FIG. 2

FLOW REGIONS OF A WING EXTENDING THROUGH MULTIPLE JETS

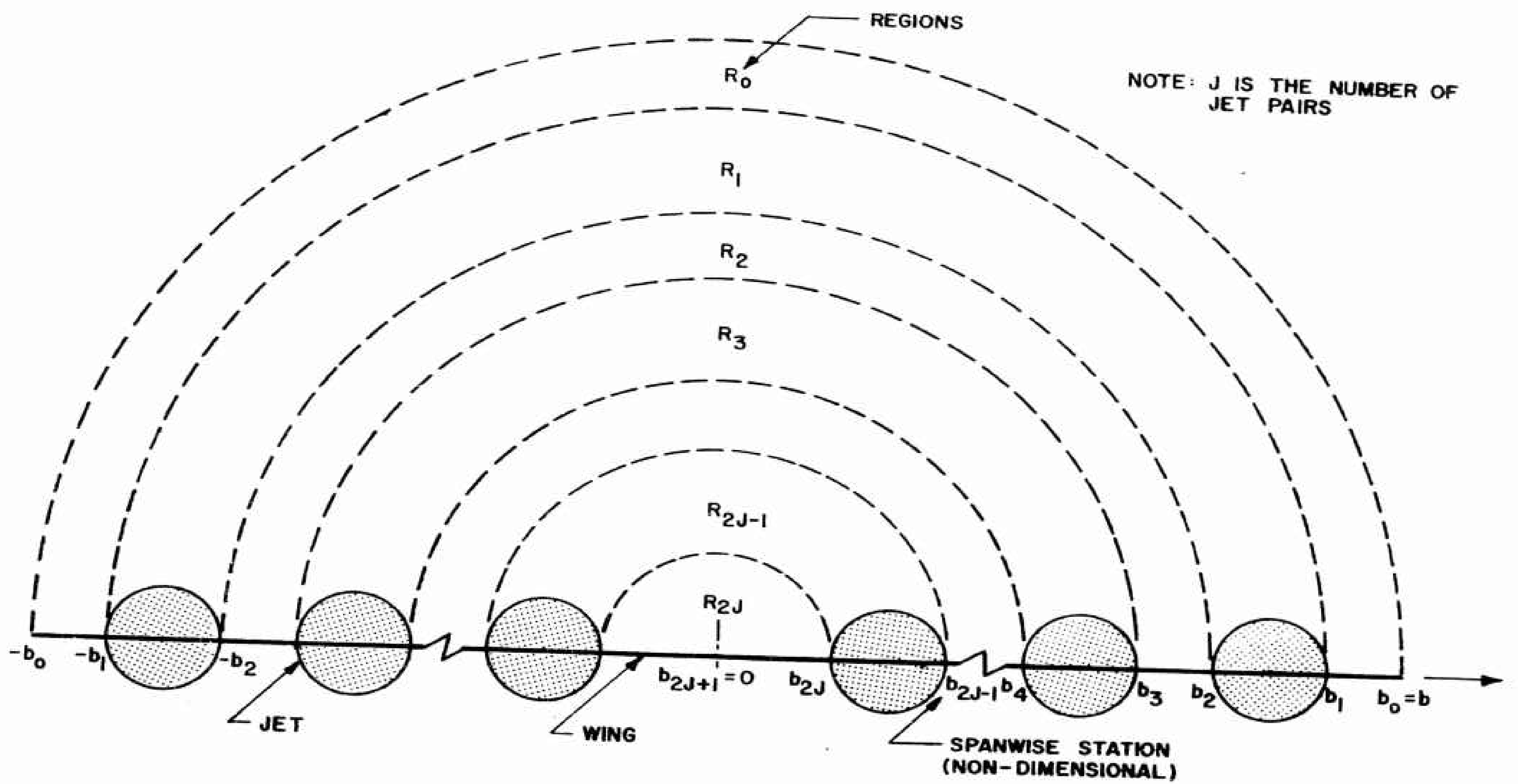

FIG. 3

SPANWISE LIFT DISTRIBUTION

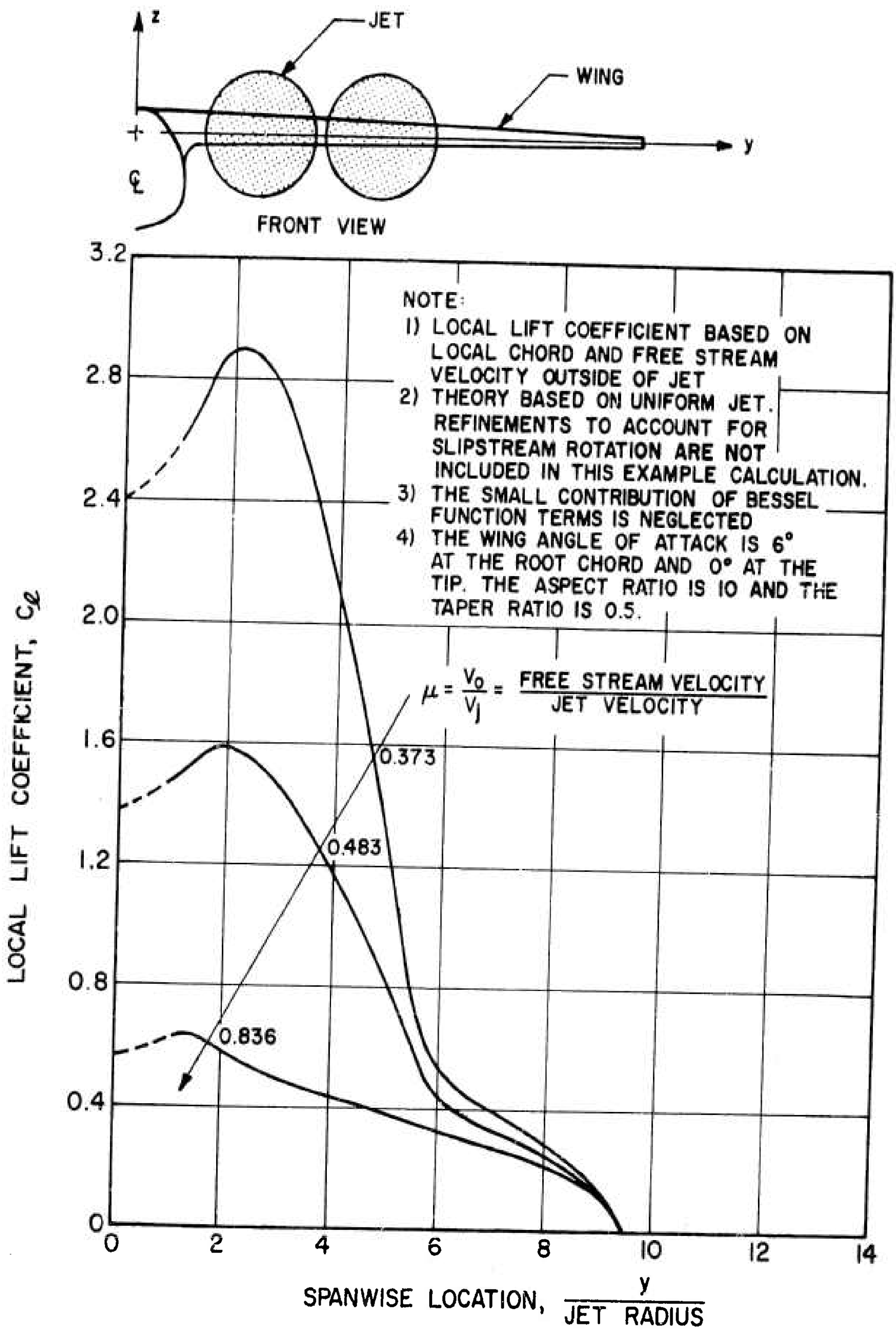

FIG. 4

DISTRIBUTION LIST

Chief, Bureau of Naval Weapons
(RAAD-3)
Department of the Navy
Washington 25, D.C.

Chief, Bureau of Naval Weapons
(RA-4)
Department of the Navy
Washington 25, D. C.

Chief, Bureau of Naval Weapons
(RR-25)
Department of the Navy
Washington 25, D.C.

Chief, Bureau of Naval Weapons
(RR-55)
Department of the Navy
Washington 25, D.C.

Commanding Officer and Director
David Taylor Model Basin
Aerodynamics Laboratory
Washington 7, D.C.

Chief of Naval Operations (OP-07T)
Department of the Navy
Washington 25, D. C.

Chief of Naval Research (Code 461)
Department of the Navy
Washington 25, D.C.
(4 copies)

Commanding Officer
Office of Naval Research Branch Office
Navy #100, Box #39, F.P.O.
New York, New York
ATTN: Head, Documents Section
(2 copies)

Commanding Officer
Office of Naval Research Branch Office
346 Broadway
New York 13, New York

Commanding Officer
Office of Naval Research Branch Office
The John Crerar Library Building
86 E. Randolph Street
Chicago 1, Illinois

Commanding Officer
Office of Naval Research Branch Office
1030 E. Green Street
Pasadena, California

Director
Naval Research Laboratory
Technical Information Office
Washington 25, D.C.
(6 copies)

Commandant of the Marine Corps
Code AAP
Arlington Annex
Washington 25, D.C.

Marine Corps Development Center
Marine Corps School
Quantico, Virginia
ATTN: Air Section

U.S. Air Force (SRGL)
Office of Scientific Research
Washington 25, D.C.

Wright Air Development Division
Directorate of Systems Management
(WWZT)
Wright-Patterson A.F.B., Ohio

Wright Air Development Division
Advanced Systems Technology(WWRPS)
Wright-Patterson A.F.B., Ohio

Office of Chief of Transportation
(TAFO-R)
Department of the Army
Washington 25, D.C.
(2 copies)

Commanding Officer
U.S. Army Transportation Research
Command (TCREC-AD)
Fort Eustis, Virginia
(2 copies)

Office, Chief of Research and
Development
Department of the Army
Washington 25, D.C.
ATTN: Air Mobility Division

Commanding General
Headquarters, Continental Army
Command
Fort Monroe, Virginia
ATTN: ATDEV-6

Commanding General
The Army Aviation Center
Combat Development Group
Fort Rucker, Alabama

Armed Services Technical Information
Agency
Document Service Center
Arlington Hall Station
Arlington 12, Virginia
(5 copies)

National Aeronautics & Space
Administration
1512 H Street, N.W.
Washington 25, D.C.
ATTN: Mr. Jack D. Brewer, Code RAA
(2 copies)

National Aeronautics & Space
Administration
Langley Research Center
Langley A.F.B., Virginia
ATTN: Mr. Donnelly

National Aeronautics and Space
Administration
Ames Research Center
Moffett Field, California
ATTN: Mr. C.W. Harper

Office, Director of Defense (R & E)
Washington 25, D.C.
ATTN: Director of Aeronautics

Office of Technical Services
Department of Commerce
Washington 25, D.C.

Library
Institute of Aeronautical Sciences
2 East 64th Street
New York 21, New York

University of Virginia
Aeronautical Engineering Department
Charlottesville, Virginia
ATTN: Dr. G.B. Matthews

Vidya, Inc.
2626 Hanover Street
Stanford Industrial Park
Palo Alto, California

Brooklyn Polytechnic Institute
Aerodynamics Laboratory
527 Atlantic Avenue
Freeport, L.I., New York

Brown University
Division of Engineering
Providence, Rhode Island
ATTN: Dr. Paul Meeder

California Institute of Technology
Aeronautics Department
Pasadena, California
ATTN: Dr. Clark Millikan

Agricultural & Mechanical College
of Texas
Aeronautical Engineering Department
College Station, Texas
ATTN: Prof. F. Weick

University of Washington
Department of Aeronautical Engineering
Seattle 5, Washington
ATTN: Prof. F.S. Eastman

University of Wichita
Department of Engineering Research
Wichita 14, Kansas
ATTN: Dean K. Razak

Aerophysics Corporation
17 Dupont Circle
Washington 6, D.C.
ATTN: Dr. G. Boehler

Armour Research Foundation
3440 South State Street
Chicago, Illinois

AVCO Manufacturing Corporation
Lycoming Division
550 South Main Street
Stratford, Connecticut
ATTN: Dr. Fritz Haber

Beech Aircraft Corporation
Wichita, Kansas
ATTN: Mr. M. J. Gordon

Bell Aerosystems Company
P.O. Box 1
Buffalo 5, New York
ATTN: Advanced Design

Bell Helicopter Corporation
P.O. Box No. 482
Fort Worth 1, Texas
ATTN: Mr. B. Kelly, V.P.
Engineering

Boeing Airplane Company
Wichita, Kansas
ATTN: Mr. H. Higgens

Cessna Aircraft Company
Wallace Plant
Wichita, Kansas

Collins Radio Company
Cedar Rapids, Iowa
ATTN: Dr. A. Lippisch

Convair Division
General Dynamics Corporation
Fort Worth, Texas
ATTN: Chief Engineer

Convair Division
General Dynamics Corporation
Pomona, California

Cornell Aeronautical Laboratory, Inc.
4455 Genesee Street
Buffalo 21, New York
ATTN: Mr. H. A. Cheilek

Douglas Aircraft Company, Inc.
El Segundo Division
El Segundo, California
ATTN: Chief Engineer

Fairchild Aircraft & Missiles Division
Research Department
Hagerstown, Maryland
ATTN: Mr. R. Darby

Goodyear Aircraft Corporation
1210 Massillon Road
Akron 15, Ohio
ATTN: Dr. R. Ross

Cornell University
Graduate School of Aeronautics
Ithaca, New York
ATTN: Dr. W.R. Sears

Georgia Institute of Technology
Guggenheim School of Aeronautics
Atlanta, Georgia
ATTN: D.W. Dutton
W. Castles

The Johns Hopkins University
Applied Physics Laboratory
Baltimore 18, Maryland
ATTN: Dr. F. H. Clauser
Mr. D. W. Rabenhorst

The Johns Hopkins University
Mechanical Engineering Department
Baltimore 18, Maryland
ATTN: Dr. Stanley Corrsin

Massachusetts Institute of Technology
Aeronautical Engineering Department
Cambridge 30, Massachusetts
ATTN: Dr. R.H. Miller

Mississippi State University
Engineering and Industrial Research Station
State College, Mississippi
ATTN: Aerophysics Department

Naval Postgraduate School
Aeronautical Engineering Department
Monterey, California
ATTN: Dr. R. Head

University of Michigan
Department of Aeronautical Engineering
Ann Arbor, Michiagn
ATTN: Dr. W. Nelson

University of Minnesota
Aeronautical Engineering Department
Minneapolis 14, Minnesota
ATTN: Prof. J.A. Akerman

New York University
Aeronautical Engineering Department
New York, New York
ATTN: Dr. Lee Arnold

Technological Institute
Northwestern University
Mechanical Engineering Department
Evanston, Illinois
ATTN: Prof. A.B. Cambel

Ohio State University
Department of Aeronautical Engineering
Columbus, 10, Ohio
ATTN: Prof. G.L. vonEschen

Princeton University
Aeronautical Engineering Department
James Forrestal Research Center
Princeton, New Jersey
ATTN: Prof. D.C. Hazen
Prof. A.A. Nikolsky

Purdue University
Aeronautical Engineering Department
Lafayette, Indiana

Rensselaer Polytechnic Institute
Aeronautical Engineering Department
Troy, New York

Stanford University
Guggenheim School of Aeronautics
Stanford, California
ATTN: Prof. E.G. Reid

Stevens Institute of Technology
Fluid Dynamics Laboratory
Hoboken, New Jersey
ATTN: Mr. L. H. Mott

Syracuse University
Mechanical Engineering Department
Syracuse, New York
ATTN: Dr. S. Eskinasi

Grumman Aircraft Engineering Corp.
Bethpage, L.I., New York
ATTN: Dr. C.E. Mack, Chief, Research
Mr. F.T. Kurt

Hiller Aircraft Corporation
Advanced Research Division
1350 Willow Road
Palo Alto, California
ATTN: Dr. J. Sissingh

Hughes Tool Company
Aircraft Division
Culver City, California
ATTN: Chief Engineer

Kaman Aircraft Corporation
Old Windsor Road
Bloomfield, Connecticut
ATTN: Mr. J. Thomas

Lockheed Aircraft Corporation
Georgia Division
86 S. Cobb Drive
Marietta, Georgia

The Martin Company
Baltimore 3, Maryland
ATTN: Chief Engineer

McDonnell Aircraft Corporation
St. Louis, Missouri
ATTN: Chief Engineer

North American Aviation, Inc.
Columbus Division
Columbus 16, Ohio

Northrup Aircraft, Inc.
Hawthorne, California
ATTN: Dr. W. Pfenninger

Piasecki Aircraft Corporation
Island Road, International Airport
Philadelphia 42, Pennsylvania
ATTN: Chief Engineer

Republic Aviation Corporation
Farmingdale, L.I., New York
ATTN: Chief Engineer

Ryan Aeronautical Company
Lindbergh Field
San Diego, California
ATTN: Chief Engineer

Therm, Inc.
Ithaca, New York
ATTN: Dr. Ritter

United Aircraft Corporation
Hamilton Standard Division
Windsor Locks, Connecticut
ATTN: Mr. G. Rosen

Pratt & Whitney Division
United Aircraft Corporation
400 Main Street
East Hartford, Connecticut

Vehicle Research Corporation
1661 Lombardy Road
Pasadena, California
ATTN: Dr. Scott Rethorst

Vertol Division, Boeing Airplane Co.
Woodland Avenue
Morton, Pennsylvania
ATTN: Mr. L.L. Douglas

VEHICLE RESEARCH CORPORATION, REPORT NO. 8
A LIFTING SURFACE THEORY FOR WINGS EXTENDING THROUGH MULTIPLE JETS. T. Yao-tsu Wu, Richard B. Talmadge. August 1961.

The basic Rethorst lifting surface solution of a wing extending through a single jet was generalized to enhance its applicability to the solution of many general and secondary problems concerned with the non-uniform aerodynamics of wing-propeller interaction. The generalization is first developed in detail in terms of single jet theory. Then it is applied to multi-jet arrangements.

Several significant refinements to the original Rethorst theory are introduced. The wing is represented by a distribution of infinitesimal vortex elements instead of a large but finite number of horseshoe vortices. Certain symmetry restrictions are removed and the effect of slipstream rotation is included.

The spanwise lift distribution of an example multi-jet arrangement was determined. Large increases in lift inboard and within the jets were obtained when the free stream velocity was small compared to the jet velocity. A lesser but significant increase occurred outboard of the jets.

This large lift magnification offers the potential of large improvements in STOL capabilities and warrants a further computational effort which is presently being conducted.

1. Incompressible Flow (1.1.1)
2. Wing Theory (1.2.2.1)
3. Propeller Slipstreams (1.5.4)
4. Aircraft Performance (1.7.1.3)

I. Wu, T. Yao-tsu
II. Talmadge, Richard B.
III. Vehicle Research Corporation Report No. 8

VEHICLE RESEARCH CORPORATION, REPORT NO. 8
A LIFTING SURFACE THEORY FOR WINGS EXTENDING THROUGH MULTIPLE JETS. T. Yao-tsu Wu, Richard B. Talmadge. August 1961.

The basic Rethorst lifting surface solution of a wing extending through a single jet was generalized to enhance its applicability to the solution of many general and secondary problems concerned with the non-uniform aerodynamics of wing-propeller interaction. The generalization is first developed in detail in terms of single jet theory. Then it is applied to multi-jet arrangements.

Several significant refinements to the original Rethorst theory are introduced. The wing is represented by a distribution of infinitesimal vortex elements instead of a large but finite number of horseshoe vortices. Certain symmetry restrictions are removed and the effect of slipstream rotation is included.

The spanwise lift distribution of an example multi-jet arrangement was determined. Large increases in lift inboard and within the jets were obtained when the free stream velocity was small compared to the jet velocity. A lesser but significant increase occurred outboard of the jets.

This large lift magnification offers the potential of large improvements in STOL capabilities and warrants a further computational effort which is presently being conducted.

1. Incompressible Flow (1.1.1)
2. Wing Theory (1.2.2.1)
3. Propeller Slipstreams (1.5.4)
4. Aircraft Performance (1.7.1.3)

I. Wu, T. Yao-tsu
II. Talmadge, Richard B.
III. Vehicle Research Corporation Report No. 8

VEHICLE RESEARCH CORPORATION, REPORT NO. 8
A LIFTING SURFACE THEORY FOR WINGS EXTENDING THROUGH MULTIPLE JETS. T. Yao-tsu Wu, Richard B. Talmadge. August 1961.

The basic Rethorst lifting surface solution of a wing extending through a single jet was generalized to enhance its applicability to the solution of many general and secondary problems concerned with the non-uniform aerodynamics of wing-propeller interaction. The generalization is first devaloped in detail in terms of single jet theory. Then it is applied to multi-jet arrangements.

Several significant refinements to the original Rethorst theory are introduced. The wing is represented by a distribution of infinitesimal vortex elements instead of a large but finite number of horseshoe vortices. Certain symmetry restrictions are removed and the effect of slipstream rotation is included.

The spanwise lift distribution of an example multi-jet arrangement was determined. Large increases in lift inboard and within the jets were obtained when the free stream velocity was small compared to the jet velocity. A lesser but significant increase occurred outboard of the jets.

This large lift magnification offers the potential of large improvements in STOL capabilities and warrants a further computational effort which is presently being conducted.

1. Incompressible Flow (1.1.1)
2. Wing Theory (1.2.2.1)
3. Propeller Slipstreams (1.5.4)
4. Aircraft Performance (1.7.1.3)

I. Wu, T. Yao-tsu
II. Talmadge, Richard B.
III. Vehicle Research Corporation Report No. 8

VEHICLE RESEARCH CORPORATION, REPORT NO. 8
A LIFTING SURFACE THEORY FOR WINGS EXTENDING THROUGH MULTIPLE JETS. T. Yao-tsu Wu, Richard B. Talmadge. August 1961.

The basic Rethorst lifting surface solution of a wing extending through a single jet was generalized to enhance its applicability to the solution of many general and secondary problems concerned with the non-uniform aerodynamics of wing-propeller interaction. The generalization is first developed in detail in terms of single jet theory. Then it is applied to multi-jet arrangements.

Several significant refinements to the original Rethorst theory are introduced. The wing is represented by a distribution of infinitesimal vortex elements instead of a large but finite number of horseshoe vortices. Certain symmetry restrictions are removed and the effect of slipstream rotation is included.

The spanwise lift distribution of an example multi-jet arrangement was determined. Large increases in lift inboard and within the jets were obtained when the free stream velocity was small compared to the jet velocity. A lesser but significant increase occurred outboard of the jets.

This large lift magnification offers the potential of large improvements in STOL capabilities and warrants a further computational effort which is presently being conducted.

1. Incompressible Flow (1.1.1)
2. Wing Theory (1.2.2.1)
3. Propeller Slipstreams (1.5.4)
4. Aircraft Performance (1.7.1.3)

I. Wu, T. Yao-tsu
II. Talmadge, Richard B.
III. Vehicle Research Corporation Report No. 8

VEHICLE RESEARCH CORPORATION, REPORT NO. 8
A LIFTING SURFACE THEORY FOR WINGS EXTENDING THROUGH MULTIPLE JETS. T. Yao-tsu Wu, Richard B. Talmadge. August 1961.

The basic Rethorst lifting surface solution of a wing extending through a single jet was generalized to enhance its applicability to the solution of many general and secondary problems concerned with the non-uniform aerodynamics of wing-propeller interaction. The generalization is first developed in detail in terms of single jet theory. Then it is applied to multi-jet arrangements.

Several significant refinements to the original Rethorst theory are introduced. The wing is represented by a distribution of infinitesimal vortex elements instead of a large but finite number of horseshoe vortices. Certain symmetry restrictions are removed and the effect of slipstream rotation is included.

The spanwise lift distribution of an example multi-jet arrangement was determined. Large increases in lift inboard and within the jets were obtained when the free stream velocity was small compared to the jet velocity. A lesser but significant increase occurred outboard of the jets.

This large lift magnification offers the potential of large improvements in STOL capabilities and warrants a further computational effort which is presently being conducted.

1. Incompressible Flow (1.1.1)
2. Wing Theory (1.2.2.1)
3. Propeller Slipstreams (1.5.4)
4. Aircraft Performance (1.7.1.3)

I. Wu, T. Yao-tsu
II. Talmadge, Richard B.
III. Vehicle Research Corporation Report No. 8

VEHICLE RESEARCH CORPORATION, REPORT NO. 8
A LIFTING SURFACE THEORY FOR WINGS EXTENDING THROUGH MULTIPLE JETS. T. Yao-tsu Wu, Richard B. Talmadge. August 1961.

The basic Rethorst lifting surface solution of a wing extending through a single jet was generalized to enhance its applicability to the solution of many general and secondary problems concerned with the non-uniform aerodynamics of wing-propeller interaction. The generalization is first developed in detail in terms of single jet theory. Then it is applied to multi-jet arrangements.

Several significant refinements to the original Rethorst theory are introduced. The wing is represented by a distribution of infinitesimal vortex elements instead of a large but finite number of horseshoe vortices. Certain symmetry restrictions are removed and the effect of slipstream rotation is included.

The spanwise lift distribution of an example multi-jet arrangement was determined. Large increases in lift inboard and within the jets were obtained when the free stream velocity was small compared to the jet velocity. A lesser but significant increase occurred outboard of the jets.

This large lift magnification offers the potential of large improvements in STOL capabilities and warrants a further computational effort which is presently being conducted.

1. Incompressible Flow (1.1.1)
2. Wing Theory (1.2.2.1)
3. Propeller Slipstreams (1.5.4)
4. Aircraft Performance (1.7.1.3)

I. Wu, T. Yao-tsu
II. Talmadge, Richard B.
III. Vehicle Research Corporation Report No. 8

VEHICLE RESEARCH CORPORATION, REPORT NO. 8
A LIFTING SURFACE THEORY FOR WINGS EXTENDING THROUGH MULTIPLE JETS. T. Yao-tsu Wu, Richard B. Talmadge. August 1961.

The basic Rethorst lifting surface solution of a wing extending through a single jet was generalized to enhance its applicability to the solution of many general and secondary problems concerned with the non-uniform aerodynamics of wing-propeller interaction. The generalization is first developed in detail in terms of single jet theory. Then it is applied to multi-jet arrangements.

Several significant refinements to the original Rethorst theory are introduced. The wing is represented by a distribution of infinitesimal vortex elements instead of a large but finite number of horseshoe vortices. Certain symmetry restrictions are removed and the effect of slipstream rotation is included.

The spanwise lift distribution of an example multi-jet arrangement was determined. Large increases in lift inboard and within the jets were obtained when the free stream velocity was small compared to the jet velocity. A lesser but significant increase occurred outboard of the jets.

This large lift magnification offers the potential of large improvements in STOL capabilities and warrants a further computational effort which is presently being conducted.

1. Incompressible Flow (1.1.1)
2. Wing Theory (1.2.2.1)
3. Propeller Slipstreams (1.5.4)
4. Aircraft Performance (1.7.1.3)

I. Wu, T. Yao-tsu
II. Talmadge, Richard B.
III. Vehicle Research Corporation Report No. 8

VEHICLE RESEARCH CORPORATION, REPORT NO. 8
A LIFTING SURFACE THEORY FOR WINGS EXTENDING THROUGH MULTIPLE JETS. T. Yao-tsu Wu, Richard B. Talmadge. August 1961.

The basic Rethorst lifting surface solution of a wing extending through a single jet was generalized to enhance its applicability to the solution of many general and secondary problems concerned with the non-uniform aerodynamics of wing-propeller interaction. The generalization is first developed in detail in terms of single jet theory. Then it is applied to multi-jet arrangements.

Several significant refinements to the original Rethorst theory are introduced. The wing is represented by a distribution of infinitesimal vortex elements instead of a large but finite number of horseshoe vortices. Certain symmetry restrictions are removed and the effect of slipstream rotation is included.

The spanwise lift distribution of an example multi-jet arrangement was determined. Large increases in lift inboard and within the jets were obtained when the free stream velocity was small compared to the jet velocity. A lesser but significant increase occurred outboard of the jets.

This large lift magnification offers the potential of large improvements in STOL capabilities and warrants a further computational effort which is presently being conducted.

1. Incompressible Flow (1.1.1)
2. Wing Theory (1.2.2.1)
3. Propeller Slipstreams (1.5.4)
4. Aircraft Performance (1.7.1.3)

I. Wu, T. Yao-tsu
II. Talmadge, Richard B.
III. Vehicle Research Corporation Report No. 8